

1 Response to Referee # 1

2 AC: The authors thank anonymous referee #1 for the detailed and constructive review of  
3 our manuscript. We agree with the referee that the manuscript would be improved by  
4 major revisions to the data analysis sections. The manuscript has now undergone a major  
5 revision, which includes a rewriting of the majority of the results section in order to give  
6 a more balanced presentation of the results. We think that the major revision in response  
7 to these referee comments has strongly improved the manuscript presentation. We thank  
8 the referee for carefully itemizing each concern and below we respond to each item with  
9 an explanation about the changes made to address each point.

10 *RC: The study can become publishable without new simulations, but I want to stress that*  
11 *this requires a careful re-analysis of the data and completely rewriting the results section*  
12 *so that it truthfully reflects the data.*

13 AC: The analysis section of the manuscript (Section 3) has been rewritten. Revised text is  
14 highlighted in red. The focus of this rewriting was to provide a more balanced and  
15 complete presentation related to the model-model and model-measurement comparisons.  
16 To assist with interpretation of the results in a more quantitative framework, we  
17 conducted calculations of the bias and error (Eqs. 6-8) between model and measurements.  
18 These results are presented in the new Tables 2-5 and are used in the revised discussion  
19 of Figs. 3-6. Please note that we have removed the original Fig. 2 as we agreed with the  
20 referee that this figure was redundant to the information presented in Fig.1. As a result,  
21 the old Figs. 4 and 5 are now Figs. 3 and 4. As well we removed Appendix Figure A1 as  
22 being redundant with Fig. 1. As well, please note that Figs. 3 and 5 include a correction  
23 that is particularly evident in summer. We had erroneously truncated the size distributions  
24 at 10 nm as opposed to 20 nm for the original Alert figures (original Figs 4 and 6). This  
25 error is corrected in the revised Figs. 3 and 5.

26 *RC: 1. Fig 4 and 5.: The following statement is simply not true: “Of the four simulations,*  
27 *NEWSCAV+COAG provides the closest agreement with the measurements at both sites*  
28 *and for all seasons”. For example, NONUC gives a better match in autumn for both sites.*  
29 *At Zeppelin (and for large part of the size distribution also at Alert), NEWS- CAV gives a*  
30 *better match in summer.*

31 AC: Following our reanalysis, we have removed this statement. We calculated the model-  
32 measurement fractional bias (Eq. 6 in text) for each of the four simulations over two  
33 particle-diameter ranges shown in Figs. 3 and 4 (20-100 nm and 100-500 nm). The new  
34 Tables 2 and 3 give these bias values. We use red/bold highlights in each table to indicate  
35 the simulation with the fractional bias value closest to zero. These tables indicate (as the  
36 referee noted) that NEWSCAV does perform better than NEWSCAV+COAG in summer  
37 at Zeppelin for both size ranges. As well NONUC is best in autumn for both size ranges  
38 and at both sites. These points are discussed in the revised text. We also added discussion  
39 to indicate that NONUC may be right but for the wrong reasons. Shutting off all new-  
40 particle formation may compensate for errors in the wet removal or coagulation sink  
41 terms.

42 *RC: 2. Fig. 6 and 7: “Among our four simulations, the simulation NEWSCAV+COAG*  
43 *yields the closest agreement with the integrated number measurements (N20, N80, N200)*  
44 *in all seasons at both sites.” I’m extremely confused by this statement, as it is so*  
45 *obviously untrue. Are we not looking at the same figures?*

46 AC: Following the data reanalysis, we have removed this statement. As the new Tables 4  
47 and 5 indicate, NONUC does perform best among the four simulations at Zeppelin for the  
48 N20, N80 and N200 in terms of the mean fractional bias (Eq. 7 in text), although the  
49 performance in terms of the mean fractional error (Eq. 8 in text) is best for  
50 NEWSCAV+COAG at Zeppelin. This is included in our revised discussion. We also  
51 include discussion about the MFB and MFE at Alert being closest to zero for N20 and  
52 N80 for NEWSCAV+COAG, but NONUC performing better for N200 MFB and MFE at  
53 Alert.

54 *RC: 3. Fig 4 and 5: The following statement is not true for all seasons: “Among our four*  
55 *simulations, the NEWSCAV+COAG simulation gives the closest representation of the*  
56 *number of non-summer Aitken and accumulation mode aerosols relative to the in-situ*  
57 *measurements at both Alert and Mt. Zeppelin.” For example, during autumn (SON), both*  
58 *figures indicates better match for both modes with NONUC. At Zeppelin, also STD seems*  
59 *to capture the Aitken mode number better. At Alert in DJF, NONUC may also perform*  
60 *better for accumulation mode (difficult to say exactly without access to numerical data).*  
61 *These facts must be mentioned.*

62 AC: The above statement is removed following the rewriting of the results section. As  
63 indicated in our reply to RC: 1 above, we added a discussion about the best performance  
64 of NONUC in autumn at both sites and this is also shown in Tables 2 and 3. We did find  
65 for the accumulation mode that NONUC performed best in winter at Alert and also  
66 Zeppelin and this is noted in red in Tables 2 and 3 and part of the revised discussion.

67 *RC: 4. The following statement is misleading: “Figures 4 and 5 show that in summer, the*  
68 *simulations NEWSCAV and NEWSCAV+COAG capture the dominant Aitken mode.” For*  
69 *Zeppelin, STD captures this features in practice just as well. Further down page 29092,*  
70 *one should stress that both NEWSCAV and NEWSCAV+COAG \*strongly\* over- estimate*  
71 *particle number below 30 nm (actually 40 nm for NEWSCAV) at Alert.*  
72

73 AC: The above statement is removed in the revised text. The text now discusses that the  
74 particle number is strongly overestimated at Alert for sizes smaller than 40 nm (and  
75 underestimated from 40-100 nm). We also note the need for care in interpreting the  
76 fractional bias values over this range where errors of over and under prediction will  
77 cancel over a given size range. For Zeppelin in summertime, we found that NEWSCAV  
78 gave the best match to the Aitken mode based on the bias values and this is included in  
79 the revised discussion and shown by Tables 2-3.

80 *RC: 5. Fig 4 and 5: It is true that NEWSCAV improves the match with measured*  
81 *accumulation mode number (> 100 nm) most in the summer. However, the fact that it*  
82 *improves the match with the observed number of particles larger than 200 nm also in*

83 *some other seasons is very significant for correctly simulating the aerosol direct effect,*  
84 *and thus deserves a mention.*

85 AC: We agree that this improved match with measurements of particles larger than 200  
86 nm for NEWS-CAV in other non-summer seasons should be mentioned and we added this  
87 discussion. This highlights the control of wet removal on the accumulation mode  
88 throughout the annual cycle as we now emphasize in our revised discussion.

89 *RC: 6. Fig 4 and 5: “Thus, errors in the new-particle formation processes cannot*  
90 *account for the non-summer Aitken mode overprediction —“ True that it cannot account*  
91 *for all, but it clearly could account for a lot (if not the majority) of it.*

92 AC: This statement is removed in the revised text. We acknowledge in the revised text  
93 that new-particle formation and growth can play a role in the Aitken mode over  
94 prediction. As part of our related discussion, we state in Section 3.2 that ‘The balance of  
95 these processes of NPF, growth, and wet removal is a challenge for Arctic simulations of  
96 number and size. Among the four simulations and in all seasons at both sites (except for  
97 summer at Mt. Zeppelin), NEWS-CAV strongly overestimates the number of 20-40 nm  
98 diameter particles.’.

99 *RC: 7. Fig 6 and 7: This statement is not true for Zeppelin: “The summertime minimum*  
100 *in N200 is over-predicted by about a factor of two for simulation STD. Wet removal*  
101 *revisions for simulation NEWS-CAV yield a factor of two reduction to give very close*  
102 *(within 20 %) agreement with the measurements).”*

103 AC: This statement is not included in the revised discussion.

104 *RC: 8. Fig 6 and 7: “The simulation NEWS-CAV+COAG has the closest agreement with*  
105 *the seasonal cycle in the measurements.” At Alert, NEWS-CAV also performs similarly*  
106 *well (in summer even better), which should be acknowledged.*

107 AC: In regard to the old Figs 6 and 7 (now Figs. 5 and 6), the Tables 4-5 and revised text  
108 now acknowledges when NONUC and NEWS-CAV performs better than  
109 NEWS-CAV+COAG. Please note that the original version of this figure for Alert, we had  
110 erroneously plotted the N10 as opposed to the N20 for Alert. This error is corrected in the  
111 revised figure.

112 *RC: 9. Fig 6 and 7: “STD also over-predicts the summertime effective diameter by about*  
113 *a factor of two” Not true for Zeppelin.*

114 AC: We have revised the text to read the text to read ‘The simulations over-predict the  
115 aerosol effective diameter in July and August, except for NEWS-CAV at Mt. Zeppelin.’  
116 As well, Tables 4 and 5 quantify the mean fractional bias and error for the simulation  
117 relative to measurements over the annual cycle.

118 *RC: 10. It should be stated more clearly what new knowledge this study contributes to*  
119 *our understanding of the Arctic aerosol cycles. For example, the importance of transport*  
120 *and accumulation of pollution in the spring months as well as of the summertime removal*  
121 *processes has been well known for a long time. On the other hand, interstitial*  
122 *coagulation has previously reached much less attention.*

123 AC: We agree with this suggestion that the presentation would be helped by a greater  
124 emphasis on the new knowledge that the study contributes. We have made changes  
125 throughout the text in response to this comment. As there has been much attention on the  
126 spring-summer period, we point out in the introduction that our study is unique in  
127 considering number and size distribution over the entire annual cycle. “To our  
128 knowledge, ours is the first global modeling study to consider the complete annual cycle  
129 in Arctic aerosol number and size. “We also now use the word ‘annual’ as opposed to  
130 ‘seasonal’ in the title and throughout the text to emphasize the focus on the complete  
131 annual cycle. Further to this, we place a greater emphasis on the importance of the  
132 coagulation mechanism by giving this greater focus in the abstract and introduction  
133 starting with the comment ‘While the importance of wet removal is been known, there  
134 has been relatively less attention given to coagulation of interstitial particles in clouds,  
135 which is an important sink process for the number of particles smaller than about 200  
136 nm.’ and also emphasize the development in Section 3.2.

137 *RC: 11. Intro: P29081, L2: How does the climate impact of aerosols strongly depend on*  
138 *the mass distribution (in addition to number and size distribution)? L13-17: Tunved was*  
139 *hardly the first one proposing this.*

140 AC: The word ‘mass’ has been removed as redundant and the text reads as ‘The climate  
141 impact of aerosols strongly depends on aerosol number and size distributions.’ We did  
142 not mean to suggest that Tunved et al. were the first to propose these controls on the  
143 number and size distribution. We added the following sentence, ‘This inter-seasonal  
144 transition from spring to summer has been extensively studied; evidence suggests control  
145 by changes in aerosol wet removal efficiency and transport patterns (e.g. Korhonen et al.,  
146 2008, Garrett et al., 2010, Sharma et al., 2013).’ Thus we indicate work dating back to  
147 2008 related to proposed controls on the spring-summer transition.

148 *RC: 12. P29082, L 25: “through stainless steel” – missing word (inlet)? P 29083-4: The*  
149 *description of Alert site instrumentation is much more detailed than that of Zeppelin site -*  
150 *> harmonize*

151 AC: Thank you for noticing this error – we added the word ‘tubing’ here. We have also  
152 added further details about the instrumentation at Zeppelin in Section 2.2 in order to  
153 match better with the level of detail in the Alert description.

154 *RC: 13. Section 2.3: Which model levels are used in comparison? Zeppelin is located on a*  
155 *mountain on an island and thus shouldn’t be compared to model surface layer results.*

156 AC: We use the model level at about 500 m for comparisons shown. This is noted in the  
157 methods (Section 2.3) ‘Simulations at Mt. Zeppelin are sampled at the station altitude of  
158 500 m.’.

159 *RC: P.29085: The validity of the nucleation mechanism is impossible to evaluate at this*  
160 *stage, since the manuscript detailing it is “in preparation” and not accessible to the*  
161 *reviewers. What seems odd is that this mechanism produces significant nucleation in*  
162 *Arctic winter months, i.e. when there is extremely little solar radiation need to produce*  
163 *sulfuric acid. Where is the sulfuric acid coming from in the model? What are the*  
164 *modelled winter-time sulfuric acid levels in the Arctic and how do they compare with*  
165 *observations/other models?*

166 AC: We have updated the citation for the nucleation mechanism as the related study is  
167 now published in GMDD. In our simulations, the nucleation (new-particle formation) that  
168 occurs in the Arctic winter occurs in the middle/upper troposphere. We added the  
169 following discussion related to Fig. 8. ‘Simulated NPF occurs in the dark Arctic  
170 wintertime since the oxidant OH is produced through reaction of ozone and volatile  
171 organic compounds, although the OH mixing ratios are three-fold less than in summer.  
172 As a result, sulphuric acid (a particle precursor vapour) can be produced though oxidation  
173 by OH of DMS and sulphur dioxide (SO<sub>2</sub>) transported into the Arctic in winter. Our  
174 simulated Arctic wintertime sulphuric acid is about 0.01 ppt near the tropopause and  
175 diminishes towards the Earth’s surface. Measurements by Möhler and Arnold (1992)  
176 indicate wintertime sulphuric acid levels in Northern Scandinavia of about 0.1 ppt near  
177 the tropopause decreasing to 0.01 ppt near the Earth’s surface, implying the true  
178 nucleation rate could be even higher.’

179 *RC: 14. Section 2.4: Eqs. 2 and 3: It is unclear how one arrives at Eq 3. There is no beta*  
180 *in Eq 2 to be replaced with Eq. 1.*

181 AC: Thank you for pointing out this omission. The equation has been corrected and beta  
182 now appears in the denominator.

183 *RC: 15. I suggest removing Fig. 2 since it adds very little (if any) additional information*  
184 *to Fig. 1. The discussion on total number concentration can be kept.*

185 AC: We agree with this suggestion and removed Fig. 2 as the information was redundant  
186 with Fig. 1, and we kept a brief comment about the total number concentration.

187 *RC: 16. P29091, L 8-9: Isn’t the summertime variability more likely to be associated with*  
188 *nucleation event and non-event days?*

189 AC: The text to discuss Fig. 1 has been revised to read ‘In Fig. 1, the magnitude between  
190 the 20th to 80th percentiles for particles smaller than 100 nm is greatest during the  
191 months of June to August when new-particle formation (NPF) processes in the Arctic  
192 boundary layer are expected to make strong and episodic contributions to the aerosol  
193 number (e.g. Korhonen et al., 2008; Leaitch et al., 2013).’.

194 *RC: 17. P29093, L4-5: “Although the over prediction of the number of 20-30 nm at Alert*  
195 *is reduced.” This is not a full sentence and it is unclear what it refers to.*

196 AC: This sentence has been removed in the revised discussion.

197 *RC: 18. P29093, L23: “This unphysical simulation. . .” NONUC is ‘unphysical’ in the*  
198 *sense that it does not include one microphysical process – but given that including this*  
199 *pro- cess doesn’t seem to capture all the physical processes either (match to observations*  
200 *isn’t super good anyway), I would not call this one simulation more unphysical than the*  
201 *others.*

202 AC: We have removed this terminology. We added discussion about how NONUC can  
203 be right for the wrong reasons due to cancelling errors in the sink terms of wet removal  
204 and coagulation with a removal of the process of new particle formation. We added this  
205 discussion to the text regarding Figs. 3 and 4.

206 *RC: 19. P29094, L1-2: What is “more than 75%” based on?*

207 AC: The revised discussion does not include this statement and we now quantify the  
208 differences between simulations using the bias metrics presented in the new Tables 2-5  
209 and defined in Eqs. 6-8.

210 *RC: 20. P29094, L16-: “The 3-fold wintertime overprediction — “ Which simulation does*  
211 *this refer to?*

212 AC: This statement does not appear in the revised text. We now use the mean fractional  
213 bias and mean fractional error as metrics for comparing the simulated N20, N80 and  
214 N200 with measurements as presented in Tables 4-5.

215 *RC: 21. P29095, L24: precursors of what?; L26-27: maxima -> maximum (or ‘maxima*  
216 *which ARE’)*

217 AC: The sentence at P29095 does not appear in the revised text. We corrected to word  
218 maxima to maximum in the following revised sentence ‘The simulated early-spring NPF  
219 rate maximum for nucleation-size particles is associated with NPF in the middle and  
220 upper troposphere, and as a result is not evident in the measurements at Alert and Mt.  
221 Zeppelin.’.

222 *RC: 22. Fig. 9: Why isn’t condensation seen as a loss process for nucleation mode (it is a*  
223 *source process for the Aitken model)? What is the logic of giving the \*inverse\* of*  
224 *accumulation or loss (black line)? I found it very confusing.*

225 AC: Condensation is a loss process for the nucleation mode but we find that coagulation  
226 is dominant such that condensation does not show up on the linear scale. As well, we re-  
227 plotted this figure (now Fig. 8) such that the sign is flipped for the net build-up or loss.

228 *RC: 23. Fig. 9: “Primary particle emissions within the Arctic account for about 10–20%*  
229 *of the source rate throughout the year in our simulation” Of the Aitken mode source*  
230 *rate? How can it be 10-20% throughout the year with such a constant emission rate and*  
231 *such a highly varying transport rate? “— dry deposition accounting for about 20– 25%*  
232 *of remaining sink.” Since dry and wet deposition seem to be the only two factors affecting*  
233 *the \*remaining sink\* (i.e. if coagulation not taken into the account), doesn’t the figure*  
234 *imply that dry deposition is responsible for more than 50% of the remaining sink?*

235 AC: The sentence regarding primary particle emissions has been revised to read ‘For the  
236 Aitken mode, simulated primary particle emissions within the Arctic have a relatively  
237 constant source rate throughout the year, quite similar in magnitude to the maximum  
238 condensational growth rate for the Aitken mode in March-April.’.

239 We revised the sentence regarding dry deposition to read ‘Coagulation is the dominant  
240 sink for the Aitken mode with dry deposition accounting for the majority of the  
241 remaining sink.’.

242 *RC: 24. What causes the minimum in the simulated size distributions around 60 nm*  
243 *(Hoppel minimum), if not cloud processing of activated particles? Here activation size to*  
244 *cloud droplets is 80 nm.*

245 AC: In our simulations, the larger of the Aitken mode particles (about 60-100 nm) do  
246 activate to form cloud droplets and are removed as precipitation forms. To avoid  
247 confusion we now state in the methods that the assumption about 80 nm is only for the  
248 purpose of the interstitial coagulation parameterization.

249 *RC: 25. Fig. 10: From which latitudes are the nucleation mode particles transported (4-*  
250 *10 km altitude) - i.e. from how far they travel without growing or coagulating? Where*  
251 *does the spring time peak transported dust come from? It is stated that “Figure 10 shows*  
252 *that the early spring-time transport occurs mainly at altitudes above 4 km, a time when*  
253 *the polar dome still extends relatively far southward.” This is not true for the coarse*  
254 *mode that is the topic of this paragraph. Perhaps the authors are talking about the other*  
255 *modes here, but since it is in no way indicated, it is impossible to know.*

256 AC: In regard to the possible latitudes of origin of the nucleation mode, we expect that  
257 there are episodes such as after scavenging when the troposphere may be very clean and  
258 particularly towards the upper troposphere such clean conditions can occur such that the  
259 lifetime of nucleation mode particles could be quite long (about one week). Thus these  
260 very small particles could be transported over considerable distances. We added this  
261 following comment about the potential for this longer lifetime with respect to  
262 coagulation, ‘At these altitudes and particularly when the atmosphere just been cleaned  
263 by a precipitation event, if the Aitken and accumulation mode concentrations are low ( $5-$   
264  $10 \text{ cm}^{-3}$ ), then nucleation-mode particles can have a lifetime of about one week with  
265 respect to loss by coagulation.’.

266 In regard to the question about springtime transport, we have revised this sentence to  
267 explicitly refer to the coarse mode, which was the topic of the paragraph. The sentence  
268 now reads ‘Figure 9 shows that the early springtime transport of the coarse mode occurs  
269 mainly at altitudes between 1.5 and 4 km, a time when the polar dome still extends  
270 relatively far southward.’

271 *RC: 26. I find Figures A2-A4 quite redundant and suggest leaving them + the one*  
272 *paragraph discussing them out. If the authors insist on keeping these figures, take them*  
273 *out of the appendix and justify their significance better.*

274 AC: We agree that some of this presentation regarding aerosol processes in other latitude  
275 ranges could be removed. For example, there are quite a few similarities between the 78N  
276 and 66N figures, and also similarities between the 50N and global figures. We decided to  
277 remove the 78N and global figures and retain the 50N figure, putting it into the main text  
278 with a discussion at the end of Section 3.3 that better justifies the significance of the  
279 figure in putting the 66N figure in context. As a result of these changes, the manuscript  
280 no longer has an appendix section.

281 *RC: 27. P29098, L16-17: there is no clear mention of latitudinal dependencies when dis-*  
282 *cussing Figs. 9 and 10.*

283 AC: This sentence is removed in the revised discussion.

284 *RC: 28. P29098 L20-21: “may be considered as the inverse of the wet removal*  
285 *efficiency” Don’t you mean “are approximated here as”? What is the logic for showing*  
286 *the wet removal lifetime for all these altitudes? At 10 km, the lifetime seems to be > 10<sup>5</sup>*  
287 *days → clearly this is not the dominant process here. To evaluate the conclusions, it*  
288 *would be important to know the corresponding lifetimes also for other processes (all*  
289 *altitude ranges)*

290 AC: This sentence is removed in the revised discussion

291 We agree that showing such an extensive set of lifetimes at many altitudes was excessive  
292 and distracting from our main point. We removed this figure and replaced the figure with  
293 the simplified Fig. 10, which better illustrates our points that 1) there is a change in  
294 accumulation aerosol number lifetime during the annual cycle and that the timing of the  
295 sharp decrease in lifetime coincides with the time when the Arctic haze layer diminishes  
296 and 2) there is a minimum in the Arctic boundary layer lifetimes in October, coincident  
297 with the total particle number minimum.

298 *RC: 29. P29098, L22-24: “This simulated aerosol lifetime with respect to wet removal*  
299 *has a summertime minimum in the Arctic for aerosols in the Aitken, accumulation and*  
300 *coarse size ranges throughout the troposphere”. Do you refer to north of 66 deg here? If*  
301 *so, the green line (closest to ground) has a minimum in the autumn, not summer.*

302 AC: These sentences are removed. The revised figure (Fig. 10) only includes two layers  
303 below 4 km and two regions (north of 50N and north of 66N) and we now state in ‘In our  
304 simulation wet removal lifetimes in the Arctic boundary layer below 1.5 km reach a  
305 minimum in October ‘.

306 *RC: 30. P29099, L4-6: Not true for coarse mode.*

307 AC: This sentence is removed in the revised discussion.

308 *RC: 31. Note: I have not reviewed the conclusions section, since I expect it to change*  
309 *significantly once the authors redo their analysis.*

310 AC: The conclusion has been extensively revised to reflect our data reanalysis. The  
311 changes are highlighted in red in the revised manuscript.

312

313 Response to Referee 2

314 AC: The authors thank anonymous referee #2 for the helpful suggestions and questions,  
315 which have led to strong improvements on our manuscript. We indicate how we have  
316 addressed each item in the responses below.

317 *RC: Overall, the manuscript is very useful and well-written. I found no major scientific*  
318 *error, but I wish the authors would present the model/model comparisons a bit more*  
319 *carefully. I recommend this work for publication after the following comments are*  
320 *addressed.*

321 AC: We agree with the referee that the manuscript would be improved by more careful  
322 model-model comparisons. To assist with making these comparisons, we quantified the  
323 bias and error (defined in the new Eqs. 6-8) between the measurements and simulations  
324 for Figs. 3-6 and presented these results in the new Tables 2-5. Please note that we also  
325 removed Fig. 2 as being redundant with Fig. 1, and as a result the original Figs. 4-7 are  
326 now Figs. 3-6. Please note that in response to the comments of referee #1, large sections  
327 of the discussion related to data analysis (Section 3) have been rewritten to provide more  
328 balanced model-measurement and model-model comparisons. Revised text is indicated in  
329 red in the updated manuscript. We think these revisions have improved the manuscript  
330 considerably since the manuscript does address several figures that contain considerable  
331 information and it is necessary to interpret this information carefully.

332 Please also note that the appendix is removed in the revised manuscript as we considered  
333 that Fig. A1 was redundant with Fig. 1. We also have moved Fig. A3 into the main text  
334 and removed A2 and 4 as being unnecessary, based on the focus of our discussion. Please  
335 also note a correction on the new Figs. 3 and 5 since we had erroneously truncated the  
336 Alert size distributions at 10 nm as opposed to 20 nm in the original Figs. 4 and 6. This  
337 correction is most evident in the summertime simulation. As well, following the

338 comments of referee 1, Fig. 10 has been revised to have a simpler, more focused  
339 presentation.

340 *RC: Page 29081, line 7. The authors jump from the global aerosol to Arctic aerosol sud-*  
341 *denly. The transition seems abrupt. Also, the motivation for studying Arctic aerosol seems*  
342 *a little weak to me. The authors should add a little bit discussion more on why*  
343 *particularly on Arctic aerosol. For example, the climate in Arctic is more sensitive to*  
344 *aerosol perturbations than other regions due to the complex positive feedback system*  
345 *there such as snow albedo feedback. This would make the transition more smooth and the*  
346 *motivation stronger.*

347 AC: Thank you for pointing out this abrupt transition in the introduction. We have  
348 revised the first paragraph of the introduction to provide clearer motivation for the  
349 reasons for studying Arctic aerosols. We now state that ‘Aerosols play an important role  
350 in the Arctic climate, and changing aerosol concentrations are believed to have  
351 contributed to the rapid Arctic warming observed over the past few decades (Shindell and  
352 Faluvegi, 2009). However, in the Arctic there are complex aerosol feedbacks and strong  
353 seasonal aerosol cycles that make study of aerosol-climate interactions particularly  
354 challenging in this remote region (Browse et al., 2012; 2015). To address a portion of  
355 this challenging puzzle, this study focuses on understanding the processes that control the  
356 Arctic aerosol number and size distributions over the entire annual cycle.’

357 *RC: Page 29091, line 18. What did the authors mean by “aerosol formation”? new*  
358 *particle formation? And by “reducing the condensation sink”? “condensation sink” on*  
359 *accumulation mode aerosols?*

360 AC: In the revised text, we consistently use the terminology ‘new-particle formation  
361 (NPF)’ as this terminology is more widely understood to refer to the process of stabilized  
362 clusters of gas molecules forming new particles. The revised text states ‘These  
363 summertime conditions favour new-particle formation (hereafter referred to as NPF) from  
364 precursor vapours within the Arctic boundary layer due to the low condensation sink for  
365 particle-precursor vapours on to existing aerosol surface area, and the low coagulation  
366 sink for newly formed, growing particles (Leitch et al., 2013; Heintzenberg et al.,  
367 2015).’

368  
369 *RC: Page 29083, line 11. What is the difference between TSI 3776 CPC and TSI 3772*  
370 *CPC?*

371 AC: We revised the text in Section 2.1 to explain that this difference relates to the aerosol  
372 size ranges measured by these instruments. The lower size limits are 4 nm and 10 nm for  
373 the TSI CPC 3775 and 3772. Please note that we had erroneously referred to a TSI CPC  
374 3776 and this is now corrected to 3775 in the revised text.

375 *RC: Page 29084, line 7. “the same instrument configuration”? the same as what? Can*  
376 *the authors also clarify which year’s data they used at Mt. Zeppelin site and Alert site?*

377 AC: We revised the sentence to indicate the instrument configuration was the same over  
378 the measurement period considered in our study. The revised text reads ‘Thus, the data  
379 used in our study (2011-2013) come from the same instrument configuration.’.

380 The revised text now states that we use measurement data from 2011-2013 for both Mt.  
381 Zeppelin and Alert. We added this information both in the abstract and in the last two  
382 paragraphs of the introduction.

383 *RC: Page 29084, line 10. What purpose is the Ni-63 neutralizer used for?*

384 AC: The neutralizer is used to apply a Boltzmann charge distribution to the particles  
385 before entering the differential mobility analyzer. We removed this sentence since we did  
386 not include a similar discussion for Alert.

387 *RC: Page 29084, line 21. “4 degrees by 5 degrees resolution”. Do the authors have any*  
388 *sense how this coarse grid resolution would affect the model results?*

389 AC: Since this study was conducted in the Arctic region, the grid boxes at this resolution  
390 are smaller than they would be in regions towards the tropics at this resolution. This  
391 increases our confidence in using the 4x5 resolution for these Arctic simulations. We  
392 added the following comment in Section 2.3 describing the model ‘All simulations use  
393 GEOS-Chem version 9.02 at 4°x5° resolution globally, corresponding to 440 km x 95 km  
394 at 80 °N.’. In any global model study, resolution plays a role in the model results and  
395 thus we agree that it is important to document the resolution used in the study.

396 *RC: Page 29085, first paragraph. Can the authors briefly clarify how they treated the*  
397 *con- densation growth and coagulation of particles in the model? I believe it would help*  
398 *readers to understand results. Did they consider the effect of nitrate or/and non-volatile*  
399 *SOA on condensation growth? on which size sections? Did they treat coagulation among*  
400 *all size sections? Or just between size sections that are next to each other?*

401 AC: We agree that adding this information would be helpful to readers in understanding  
402 the results. We added the following paragraph near the end of Section 2.3.’ Growth of  
403 simulated particles occurs by condensation of sulphuric acid and organic vapours, which  
404 we assume to be non-volatile. These vapours condense proportional to the Fuchs-  
405 corrected aerosol surface area distribution (Donahue et al., 2011, Pierce et al., 2011,  
406 Riipinen et al., 2011). Condensational growth is not a sink for aerosol number but does  
407 transfer aerosol number between size bins while increasing aerosol mass. Coagulation is  
408 an important sink for aerosol number (particularly for aerosols with diameters smaller  
409 than 100 nm), and moves aerosol mass to larger sizes. Our simulations use the Brownian  
410 coagulation scheme of Fuchs (1964), and consider coagulation between all particle  
411 sizes.’.

412  
413 *RC: Page 29085, line 25, Liu et al. (2001) is not appropriate for dry deposition, though it*  
414 *suits well for wet deposition.*

415 AC: We added a reference to Wesley (1989) for the dry deposition scheme. Thank you  
416 for noting this omission.

417 *RC: Page 29087, line 8. Is there any justification for  $1 \times 10^{-3} \text{ s}^{-1}$ ?*

418 AC: This threshold is consistent with the maximum process rates indicated in Gettleman  
419 et al. (2013). The revised text states ‘This value is consistent with the upper limit for  
420 these process rates given in Gettelman et al. (2013).’.

421  
422 *RC: Page 29088, line 12. Pierce et al. (2014) is not seen in the reference list.*

423 AC: We corrected this reference to D’Andrea et al. (2013). Thank you for noting the  
424 need for this correction.

425 *RC: Page 29091, line 8-9. This is not consistent with what the authors stated on page*  
426 *29090, line 9.*

427 AC: The sentence at page 29091, line 8-9 is removed in the revised text.

428 *RC: Page 29091, line 20. Why does wet scavenging have less control on accumulation*  
429 *mode number in the non-summer seasons than the summer season? Because of less*  
430 *precipitations?*

431 AC: This sentence is removed in the revised discussion. The revised text now indicates  
432 that wet removal has a role in controlling the accumulation mode in all seasons. However  
433 we discuss in more detail about how the efficiency of wet removal is greater in the Arctic  
434 boundary layer in the summer. In our simulations, we parameterize this process with a  
435 dependence on temperature. In non-summer seasons wet removal does occur within the  
436 Arctic but is less efficient at lower temperatures, and as well wet removal outside the  
437 Arctic does influence how much accumulation mode aerosol reaches the Arctic. We  
438 discuss this in detail in the revised Section 3.2.

439 *RC: Page 29091, line 25. “Reduces the condensation sink”. the sink of sulfuric acids?*

440 AC: This sentence is removed following the revisions. However we are careful in the  
441 revised text to explicitly state ‘the condensation sink for sulfuric acid’ where applicable.

442 *RC: Page 29092, line 26. “Not enough material to contribute to new-particle growth”.*  
443 *Did the authors consider the condensation of SOA on it?*

444 AC: In the revised model description (Section 2.3) we now state that we allow particle  
445 growth by SOA condensation, however this source may not be well represented in the  
446 Arctic. The revised text states that ‘Growth of simulated particles occurs by condensation  
447 of sulphuric acid and organic vapours, which we assume to be non-volatile’

448 *RC: Page 29093, line 7-9. Do these volatile organic compounds come from ocean as*  
449 *well? Is that possible that the deposition of Aitken mode aerosol is underestimated at*  
450 *Alert site?*

451 AC: These VOCs can come from the ocean and these sources for the Arctic are likely not  
452 well represented in the model. This is an important and complex problem for control of  
453 aerosol number and will be examined in future studies

454 In the revised text we acknowledge that there are uncertainties related to deposition of the  
455 Aitken mode. The related text reads, ‘Recent studies indicate that aerosols as small as 50  
456 nm - 60 nm can activate in the clean Arctic summertime conditions (Leaitech et al., 2013;  
457 Leaitech et al., 2015) and we likely under-estimate this removal in our simulations.’,  
458 although as the revised text indicates ‘aerosols larger than about 60 nm are removed by  
459 activation scavenging in our simulations.’

460 *RC: Page 29093, line 11. “at both sites and for all seasons”. I would say except for the*  
461 *summer season at Alert site.*

462 AC: This sentence is removed in the revised analysis.

463 *RC: Page 29093, line 12. This sentence is a digression. Also, the authors still discuss*  
464 *figures 4 and 5 in the following paragraph. I suggest removing this sentence.*

465 AC: This sentence is removed in the revised text.

466 *RC: Page 29093, line 19-21. Do the authors imply here that the overestimation of Aitken*  
467 *mode aerosol numbers can be explained by the errors in nucleation scheme (NPF)? This*  
468 *is in contrary to the statement in previous paragraph. In addition, is there any way to*  
469 *evaluate NH<sub>3</sub> in the model at Alert site? Did the authors think about the possibility that*  
470 *nucleation is actually associated with organic compounds while the model neglected*  
471 *this?*

472 AC: This sentence is removed in the revised text. However we do discuss that error in the  
473 NPF scheme can play a role in this overestimation (simulation of NPF is challenging for  
474 global model). This is likely not the entire reason for Aitken mode over prediction since  
475 when we shut off all NPF in the model, we still found over estimate of the Aitken mode  
476 in winter. Thus, coagulation also has an important role as discussed in detail in the text  
477 and there is a delicate balance between the processes of wet removal and NPF.

478 The NH<sub>3</sub> simulation near Alert is evaluated in Wentworth et al. (2016) relative to recent  
479 shipboard measurements. Unfortunately there are no NH<sub>3</sub> measurements at Alert.

480 The model does not include NPF by organic compounds. As now noted in the revised  
481 text, at present-day we have no good way of combining NPF by both organics and  
482 sulphuric acid-ammonia-water ternary schemes in a single mechanism. Recent work by  
483 Giamarelou et al. (2015) suggests that nucleation-mode particles in the Arctic are

484 predominantly ammoniated sulfates and thus we prefer to continue with the ternary  
485 scheme. We added this information to our model description for clarification about our  
486 choice of NPF scheme.

487 *RC: Page 29093, line 25-27. This is a misleading statement. The authors imply that*  
488 *aerosol nucleation is not important for non-Summer Aitken mode aerosol. This is not*  
489 *supported by Figures 4 and 5. The difference of Aitken aerosol numbers between the*  
490 *NEWSCAV simulation and the NONUC simulation is nearly as large as (or even larger*  
491 *in the Fall season) than that between the NEWSCAV simulation and the*  
492 *NEWSCAV+COAG simulation. This suggests that the nucleation may be as important*  
493 *as the in-cloud coagulation, at least a non-negligible process, for non-Summer Aitken*  
494 *mode aerosol. Also, the 20-50 nm aerosol number concentration predicted by the*  
495 *NONUC simulation is even closer to measurements than the NEWSCAV+COAG*  
496 *simulation at both sites on Fall (SON). This paper do show the importance of the*  
497 *coagulation in clouds, but it also shows the importance of nucleation.*

498 AC: We agree that NPF processes are important for control of the Aitken mode in all  
499 seasons and the above statement is removed from the revised text in this section. The  
500 revised text indicates that both NPF and coagulation have important controls on the non-  
501 summer Aitken number.

502 *RC: Figure 6. Please clarify the gray shaded region.*

503 AC: We added a sentence to the caption to indicate that this gray area bounds the 20-80<sup>th</sup>  
504 percentile.

505 *RC: Figure 7. Can the authors explain why all simulations over-predict aerosol numbers*  
506 *for JFM?*

507 AC: The simulations at Mt. Zeppelin do strongly over predict aerosol number in winter  
508 (as shown in Fig. 4 and Table 3). This is the subject on ongoing investigation as the  
509 revised text notes, the delicate balance between emissions, new particle formation,  
510 growth and wet removal is challenging to simulate in the Arctic.

511 *RC: Page 29094, line 13. This sentence is not accurate. The STD simulation captures*  
512 *measured N20 on JJA at Alert site better than the NEWSCAV+COAG simulation.*

513 AC: This sentence is removed in the revised analysis. As well, we found an error in the  
514 plotting of this N20 figure for Alert. We had plotted N10 as opposed to N20. The figure  
515 is now corrected. In the revised figure, the performance of NEWSCAV+COAG is better  
516 in JJA at Alert and is best among the four simulations in terms of the N20 mean fractional  
517 bias and mean fraction error across the entire annual cycle as shown in the new Table 4.  
518 However, we caution that these metrics across the entire annual cycle miss certain details,  
519 such as the close agreement with measurements for simulation STD in June at Alert and  
520 areas of over prediction and under prediction can cancel in the bias metrics. The revised  
521 discussion is more balanced and does point out when each of the simulation perform well.

522 As well, Table 4 does indicate that the N<sub>2</sub>O MFE and MFB for STD at Alert are second to  
523 NEWSCAV+COAG in being closest to zero (due to this reasonably good performance of  
524 STD in early summer).

525 *RC: Page 29095, line 24. Did the authors imply that most of precursors for the*  
526 *nucleation in early spring are transported from the outside Arctic? Because the authors*  
527 *stated next line that in summer there are greatest local precursor emissions.*

528 AC: The second paragraph of Section 3.3 has been revised to give a more detailed  
529 explanation about the summertime NPF occurring in the boundary layer and the  
530 springtime NPF occurring in the free troposphere in our simulations. In our simulations,  
531 NPF proceeds when the condensation sink for sulphuric acid is low but still some  
532 sulphuric acid is being produced. In spring, those precursors of sulphuric acid are likely  
533 transported in the free troposphere from lower latitudes over regions open water or  
534 pollution sources, and NPF occurs when the condensation sink is low. In summer there is  
535 more ice-free ocean within the Arctic that can emit dimethyl sulfide (a precursor for  
536 sulphuric acid) directly into the Arctic boundary layer and form sulphuric acid there.  
537 Then since the boundary layer is cleaner in summer, NPF proceeds here in our  
538 simulations. This discussion can be found in the revised second paragraph of Section 3.3.  
539

540

541 Summary of relevant changes:

542 All relevant manuscript changes are documented in the author responses above and are  
543 highlighted in red in the following revised manuscript.

544

545

546

547

548

549

550

551

552

553

554 **Processes controlling the annual cycle of Arctic aerosol**  
555 **number and size distributions**

556

557 **B. Croft<sup>1</sup>, R. V. Martin<sup>1,2</sup>, W. R. Leaitch<sup>3</sup>, P. Tunved<sup>4</sup>, T. J. Breider<sup>5</sup>,**  
558 **S. D. D'Andrea<sup>6</sup>, and J. R. Pierce<sup>6,1</sup>**

559

560 [1]{Department of Physics and Atmospheric Science, Dalhousie University, Halifax, NS,  
561 Canada}

562 [2]{Harvard-Smithsonian Center for Astrophysics, Cambridge, MA, USA}

563 [3]{Science and Technology Branch, Environment Canada, Toronto, Ontario, Canada}

564 [4]{Department of Environmental Science and Analytical Chemistry, Stockholm

565 University, Stockholm, Sweden}

566 [5]{School of Engineering and Applied Sciences, Harvard University, Cambridge, MA,  
567 USA}

568 [6]{Department of Atmospheric Science, Colorado State University, Fort Collins, CO,  
569 USA}

570

571 Correspondence to: B. Croft ([bcarlin@dal.ca](mailto:bcarlin@dal.ca))

572

573 **Abstract**

574

575 Measurements at high-Arctic sites (**Alert, Nunavut and Mt. Zeppelin, Svalbard**) during  
576 **the years 2011 to 2013** show a strong **and similar, annual** cycle in aerosol number and  
577 size **distributions**. **Each year at both sites**, the number of aerosols with diameters larger  
578 than 20 nm **exhibits a minimum in October, and two maxima**, one in spring associated  
579 with a dominant accumulation mode (**particles 100 nm to 500 nm** in diameter), and a  
580 second in summer associated with a dominant Aitken mode (**particles 20 nm to 100 nm** in  
581 diameter). Seasonal-mean aerosol effective diameter **from measurements** ranges from  
582 about 180 nm in summer to 260 nm in winter. This study interprets these **annual** cycles  
583 with the GEOS-Chem-TOMAS global aerosol microphysics model. **Important roles are**  
584 **documented for several processes (new-particle formation, coagulation scavenging in**

585 clouds, scavenging by precipitation, and transport) in controlling the annual cycle in  
586 Arctic aerosol number and size.  
587  
588 Our simulations suggest that coagulation scavenging of interstitial aerosols in clouds by  
589 aerosols that have activated to form cloud droplets strongly limits the total number of  
590 particles with diameters less than 200 nm throughout the year. We find that the minimum  
591 in total particle number in October can be explained by diminishing new-particle  
592 formation within the Arctic, limited transport of pollution from lower latitudes, and  
593 efficient wet removal. Our simulations indicate that the summertime-dominant Aitken  
594 mode is associated with efficient wet removal of accumulation-mode aerosols, which  
595 limits the condensation sink for condensable vapours. This in turn promotes new-particle  
596 formation and growth. The dominant accumulation mode during spring is associated with  
597 build up of transported pollution from outside the Arctic coupled with less-efficient wet  
598 removal processes at colder temperatures. We recommend further attention to the key  
599 processes of new-particle formation, interstitial coagulation, and wet removal and their  
600 delicate interactions and balance in size-resolved aerosol simulations of the Arctic to  
601 reduce uncertainties in estimates of aerosol radiative effects on the Arctic climate.

## 602 **1. Introduction**

603 The climate impact of aerosols strongly depends on aerosol number and size distributions  
604 (Haywood and Boucher, 2000; Lohmann and Feichter, 2005). These aerosol properties, in  
605 addition to chemical composition, contribute to aerosol effects on the Earth's  
606 climate. Aerosols influence the global climate directly through scattering and absorption  
607 of radiation (Charlson et al., 1992), and indirectly by modifying cloud properties

608 (Twomey, 1974; Albrecht, 1989). Aerosols play an important role in the Arctic climate,  
609 and changing aerosol concentrations are believed to have contributed to the rapid Arctic  
610 warming observed over the past few decades (Shindell and Faluvegi, 2009). However, in  
611 the Arctic there are complex aerosol feedbacks and strong seasonal aerosol cycles that  
612 make study of aerosol-climate interactions particularly challenging in this remote region  
613 (Browse et al., 2012; 2015). To address a portion of this challenging puzzle, this study  
614 focuses on understanding the processes that control the Arctic aerosol number and size  
615 distributions over the entire annual cycle.

616

617 Observations at Arctic sites show a strong and similar annual cycle in aerosol number and  
618 size distributions (e.g. Ström et al., 2003; Leaitch et al., 2013; Tunved et al., 2013). In the  
619 high Arctic, at Mt. Zeppelin, Svalbard, and Alert, Nunavut, Canada, the observed annual  
620 cycle in aerosol number exhibits two maxima: one in March-April associated with  
621 dominance of accumulation-mode particles and one in July associated with smaller,  
622 Aitken-mode particles. The inter-seasonal transition from accumulation-mode-dominated  
623 springtime distributions to Aitken-mode-dominated summertime distributions has been  
624 observed not only at surface sites, but also in the free troposphere (Engvall et al., 2008).  
625 This inter-seasonal transition from spring to summer has been extensively studied;  
626 evidence suggests control by changes in aerosol wet removal efficiency, new-particle  
627 formation, and transport patterns (e.g. Korhonen et al., 2008, Garrett et al., 2010, Sharma  
628 et al., 2013). More-efficient wet removal in the mid latitudes and within the Arctic in late  
629 spring and summer inhibits transport of aged accumulation-mode aerosols into the Arctic.  
630 These summertime conditions favour new-particle formation (hereafter referred to as

631 NPF) from precursor vapours within the Arctic boundary layer due to the low  
632 condensation sink for particle-precursor vapours on to existing aerosol surface area, and  
633 the low coagulation sink for newly formed, growing particles (Leitch et al., 2013;  
634 Heintzenberg et al., 2015).

635

636 Korhonen et al. (2008) conducted a pioneering global aerosol model study to interpret the  
637 processes controlling the spring-to-summer transition in Arctic aerosol number and size  
638 observed from Svalbard and the shipboard campaigns of Heintzenberg et al. (2006). The  
639 focus of that study was limited to spring-summer and the transition between these  
640 seasons. In our study, we extend the temporal scope to consider the entire annual cycle  
641 and use observations from both Svalbard and Nunavut, about 1000 kilometers apart. Over  
642 recent years, numerous studies have focused on the spring-summer transitions in aerosol  
643 mass abundance using observations and models to examine the role of transport and  
644 scavenging (Garrett et al., 2010; Garrett et al., 2011; Browse et al., 2012; DiPierro et al.,  
645 2013; Sharma et al., 2013, Stohl et al., 2013). However, there has been considerably less  
646 focus on Arctic aerosol number and size distributions. To our knowledge, ours is the first  
647 global modeling study to consider the complete annual cycle in Arctic aerosol number  
648 and size.

649

650 In this study, we examine aerosol number and size distributions over recent years (2011-  
651 2013) at the Canadian high-Arctic measurement site at Alert, Nunavut (82.5 °N) and the  
652 European site at Mt. Zeppelin, Svalbard (79 °N). We use the GEOS-Chem global  
653 chemical transport model (Bey et al., 2001; [www.geos-chem.org](http://www.geos-chem.org)) with the size-resolved  
654 aerosol microphysics package TOMAS (D'Andrea et al., 2013; Pierce et al., 2013;

655 Trivitayanurak et al., 2008) to examine the relative importance of various aerosol  
656 processes (NPF, emissions, removal, and microphysical processes such as condensation  
657 and coagulation) in controlling the annual cycle of aerosol number and size distribution in  
658 the Arctic.

659

660 While the importance of wet removal is well known (Korhonen et al., 2008; Garrett et al.,  
661 2010; Browse et al., 2012), relatively less attention has been given to coagulation of  
662 interstitial particles in clouds, which is another sink process for aerosol number. We  
663 implemented a mechanism in GEOS-Chem-TOMAS that represents coagulation between  
664 aerosols that have activated to form cloud droplets and interstitial aerosols (defined as  
665 particles within clouds, but outside of cloud droplets). This mechanism accounts for the  
666 ~100-fold increase in size (due to water uptake) for particles that are cloud condensation  
667 nuclei (CCN) and have activated to form cloud droplets. This size change increases the  
668 coagulation rate of smaller Aitken-mode aerosols with these larger activated aerosols.  
669 Pierce et al. (2015) showed that the inclusion of this mechanism to GEOS-Chem-  
670 TOMAS brings aerosol size distributions to closer agreement with observations, globally.  
671 Cesana et al. (2012) analyzed CALIOP retrievals using the cloud-phase detection  
672 algorithm and found that low-level liquid clouds are ubiquitous in all seasons in the  
673 Arctic. Thus, this in-cloud coagulation process is particularly relevant for the Arctic.

674

675 The following section describes the 2011-2013 high-Arctic measurements and gives an  
676 overview of the GEOS-Chem-TOMAS simulations conducted for this study. Section 3  
677 examines the monthly and seasonal mean in-situ observations of aerosol number and size  
678 from scanning mobility particle sizer (SMPS) at Alert, and differential mobility particle

679 sizer (DMPS) at Mt. Zeppelin. The GEOS-Chem-TOMAS model is used to interpret the  
680 **annual** cycle of these measurements. We subsequently present the process rates that  
681 **control** the aerosol **annual** cycles in our simulations.

## 682 **2. Method**

### 683 ***2.1. Measurements at Alert***

684 Measurements of particle size distributions at Alert have been ongoing since March 2011  
685 with the exception of a few technical interruptions. Sampling of the ambient aerosol size  
686 distribution at Alert was conducted as described by Leaitch et al. (2013). Briefly, the  
687 particles are sampled through stainless steel **tubing** with a mean residence time for a  
688 particle from outside to its measurement point of approximately 3 s. At the point of  
689 sampling, the aerosol is at a temperature (T) of approximately 293K and **the** relative  
690 humidity (RH) is <50%. **The total number concentration of particles larger than 10 nm in**  
691 **diameter at Alert is measured with a TSI 3772 Condensation Particle Counter (CPC)**  
692 **operating at a flow rate of 1 litre min<sup>-1</sup> (lpm).** The size distributions for particles from 20  
693 nm to 500 nm in diameter are measured with a TSI 3034 Scanning Mobility Particle  
694 System (SMPS), operating at a flow rate of 1 **lpm** and verified for sizing on site using  
695 mono-disperse particles of polystyrene latex and of ammonium sulphate generated with a  
696 Brechtel Manufacturing Incorporated (BMI) Scanning Electrical Mobility Spectrometer  
697 (SEMS) and for number concentrations through comparison with the TSI 3772 CPC. The  
698 Alert SMPS data are accurate to within 15%, in terms of number concentration and  
699 sizing. **The TSI 3772 CPC was initially compared with a TSI 3775 CPC temporarily**  
700 **operating at the site and measuring the number of particles with sizes larger than 4 nm.**

701 The differences between the TSI 3772 and 3775 CPC were found to be <10% when there  
702 was no evidence of particles smaller than 10 nm. The TSI 3772 CPC also compares to  
703 within 10% with the SMPS when particle sizes are large enough for all particles to be  
704 counted by both instruments (e.g. during periods of Arctic Haze).

705

## 706 **2.2. Measurements at Mt. Zeppelin**

707 The Department of Environmental Science and Analytical Chemistry, Section for  
708 Atmospheric research (ACES), Stockholm University (SU), has monitored the sub-  
709 micron aerosol number size distribution at Mt. Zeppelin since 2000 with a differential  
710 mobility particle sizer (DMPS). Today, this more-than-15-year continuous dataset  
711 constitutes one of the longest unbroken aerosol number size distribution observation  
712 series in the Arctic.

713

714 During the 15 years of operation, the DMPS system has undergone a number of  
715 modernizations. Initially a single differential mobility analyzer (DMA) system was used  
716 covering a size range between roughly 20-600 nm. A major overhaul was performed  
717 during late 2010, and since then the setup has remained unchanged, covering a size range  
718 of 5-800 nm. Thus, the data used in our study (2011-2013) come from the same  
719 instrument configuration.

720

721 This DMPS-system utilizes a custom-built twin DMA setup comprising one Vienna-type  
722 medium DMA coupled to a TSI CPC 3772 covering sizes between 25-800 nm and a  
723 Vienna-type long DMA coupled with at TSI CPC 3772 effectively covering sizes

724 between 5-60 nm. The size distributions from the two systems are harmonized on a  
725 common size grid and then merged. Both systems use a closed-loop setup. The inlet hat is  
726 a whole air inlet according to EUSAAR standard. At current setup, the inlet operates with  
727 a flow rate of about 100 lpm and consists of several stainless steel tubes. The 25 mm  
728 diameter DMPS sampling tube is in total 4.5 m long. Inside the station, the flow is split  
729 into progressively smaller tubing until reaching 1 lpm at the DMPS. Laminar flow  
730 condition applies throughout the sampling line. On the outside, the inlet temperature is  
731 kept above 273K using active heating. Inside the station the temperature increases  
732 gradually to room temperature (maximum temperature of 298K, but typically around  
733 293K). RH and T are internally monitored and measurements are at dry conditions with  
734 RH<30%. The system is regularly checked with latex spheres and flow controls. The data  
735 are manually screened and crosschecked with other available observations.

### 736 ***2.3. GEOS-Chem-TOMAS model description***

737 In this study, we use the GEOS-Chem-TOMAS model, which couples the GEOS-Chem  
738 global chemical transport model ([www.geos-chem.org](http://www.geos-chem.org), Bey et al., 2001) with the Two-  
739 Moment Aerosol Sectional (TOMAS) microphysics scheme (Adams and Seinfeld, 2002;  
740 Lee and Adams, 2012). All simulations use GEOS-Chem version 9.02 at 4°x5°  
741 resolution globally, corresponding to 440 km x 95 km at 80 °N. The model has 47 layers  
742 extending from the surface to 0.01 hPa. Simulations at Mt. Zeppelin are sampled at the  
743 station altitude of 500 m. Assimilated meteorology is from the National Aeronautics and  
744 Space Administration (NASA) Global Modelling and Assimilation Office (GMAO)  
745 Goddard Earth Observing System version 5 (GEOS-5). All simulations use meteorology  
746 and emissions for the year 2011 following 3 months spin-up at the end of 2010. GEOS-

747 Chem includes simulation of more than 50 gas-phase species including oxidants such as  
748 OH and aerosol-precursor gases such as SO<sub>2</sub> and NH<sub>3</sub>. Emissions in GEOS-Chem-  
749 TOMAS are described in Stevens and Pierce (2014). In addition, we implement seabird-  
750 colony NH<sub>3</sub> emissions from Riddick et al. (2012) with modifications for additional  
751 colonies in the Arctic region based on the on-line Circumpolar Seabird Data Portal  
752 (Seabird Information Network, 2015) as described and evaluated in Wentworth et al.  
753 (2016) and Croft et al. (submitted). Our simulations include secondary organic aerosol  
754 (SOA), both biogenic (~19 Tg yr<sup>-1</sup>) and enhanced anthropogenic non-volatile (100 Tg  
755 yr<sup>-1</sup>) spatially correlated with anthropogenic CO emissions (D'Andrea et al., 2013).

756

757 The TOMAS microphysics scheme tracks the number and mass of particles within each  
758 of 15 dry size sections. The first 13 size sections are logarithmically spaced, including  
759 aerosol dry diameters from approximately 3 nm to 1 μm, while 2 additional size sections  
760 represent aerosol dry diameters from 1 μm to 10 μm (Lee and Adams, 2012). Simulated  
761 aerosol species are sulphate, sea-spray, hydrophilic organics, hydrophobic organics,  
762 internally mixed black carbon, externally mixed black carbon, dust and water. Aerosol  
763 hygroscopic growth is a function of grid box mean relative humidity (RH) capped at  
764 99%. Simulated aerosols are treated as dry (RH=0%) for comparison with the  
765 measurements presented in this study

766

767 For these simulations, NPF is treated according to the state-of-the-science ternary H<sub>2</sub>SO<sub>4</sub>-  
768 NH<sub>3</sub>-H<sub>2</sub>O nucleation scheme described by Baranizadeh et al. (2016). The formation rate  
769 of particles at circa 1.2 nm in mass diameter is determined from a full kinetics simulation

770 by Atmospheric Cluster Dynamics Code (ACDC; Olenius et al., 2013) using particle  
771 evaporation rates based on quantum chemistry. The scheme is implemented as a  
772 comprehensive look-up table of simulated formation rates as a function of sulphuric acid  
773 and ammonia vapour concentrations, relative humidity, temperature, and condensation  
774 sink for condensable vapours (existing aerosol surface area). Growth and loss of particles  
775 with diameters smaller than 3 nm are approximated with the Kerminen et al. (2004)  
776 scheme (evaluated in TOMAS in Lee et al. (2013a)). In our simulations, we do not  
777 include NPF by organic vapours such as those arising from the oceans (O'Dowd and de  
778 Leeuw, 2007; Fu et al., 2013). Currently, no single nucleation scheme includes  
779 contributions from organics, sulphuric acid, bases, and water. As well, Giamarelou et al.  
780 (2016) found that nucleation-mode particles in the Arctic are predominantly ammonium  
781 sulphates.

782

783 Growth of simulated particles occurs by condensation of sulphuric acid and organic  
784 vapours, which we assume to be non-volatile. These vapours condense proportional to the  
785 Fuchs-corrected aerosol surface area distribution (Donahue et al., 2011, Pierce et al.,  
786 2011, Riipinen et al., 2011). Condensational growth is not a sink for aerosol number but  
787 does transfer aerosol number between size bins while increasing aerosol mass.

788 Coagulation is an important sink for aerosol number (particularly for aerosols with  
789 diameters smaller than 100 nm), and moves aerosol mass to larger sizes. Our simulations  
790 use the Brownian coagulation scheme of Fuchs (1964), and consider coagulation between  
791 all particle sizes.

792

793 In our simulations, aerosols are removed from the atmosphere by precipitation both in  
794 and below clouds (Liu et al, 2001), and also by dry deposition using a resistance in-series  
795 approach (Wesley, 1989) assuming an aerosol dry deposition velocity of  $0.03 \text{ cm s}^{-1}$  over  
796 snow and ice. Wet deposition is an important sink process for aerosols larger than about  
797 50-100 nm in diameter. The in-cloud wet scavenging parameterization in the standard  
798 GEOS-Chem-TOMAS module uses the same equations for the removal efficiency and  
799 the precipitation fraction as in the bulk-aerosol GEOS-Chem module described in Liu et  
800 al. (2001) with updates implemented by Wang et al., (2011) to account for wet removal in  
801 mixed-phase and ice clouds. The aerosol in-cloud wet removal in GEOS-Chem-TOMAS  
802 is limited to the aerosol size range that is assumed activated into cloud hydrometeors.

803

## 804 ***2.4 Simulations and revisions to model parameterizations***

805 Table 1 summarizes the four simulations conducted with the GEOS-Chem-TOMAS  
806 model. These simulations include 1) a standard, 2) updates to wet removal, 3) updates  
807 that add the process of interstitial coagulation of aerosols in clouds, and 4) a sensitivity  
808 test with no NPF. The first (simulation STD) uses the standard GEOS-Chem-TOMAS  
809 model as described above.

810

811 Simulation NEWSCAV introduces developments to the wet removal parameterization to  
812 allow for variable in-cloud water content, to implement a temperature-dependent aerosol  
813 activation fraction, and to more closely relate in-cloud aerosol scavenging to cloud  
814 fraction. The standard GEOS-Chem-TOMAS wet removal efficiency  $\beta$  for large-scale

815 clouds is based on a parameterization originally developed by Giorgi and Chameides  
816 (1986):

817

$$818 \quad \beta = k_{min} + Q/L \quad \text{Eq. 1}$$

819

820 where  $Q$  is the grid- box mean precipitation production rate [ $\text{g cm}^{-3} \text{s}^{-1}$ ] from the GEOS-5  
821 meteorological fields,  $L$  is the in-cloud liquid and ice water content [ $\text{g cm}^{-3}$ ] of the  
822 precipitating clouds (an assumed constant) and  $k_{min}$  is a constant,  $1 \times 10^{-4} \text{s}^{-1}$ . The  $k_{min}$   
823 term represents autoconversion processes that produce precipitation. The  $Q/L$  term  
824 represents accretion processes. The standard GEOS-Chem model uses a globally fixed  
825 value for  $L$  of  $1 \times 10^{-6} \text{g cm}^{-3}$ . While this value performs well for wet scavenging in a  
826 global sense (Liu et al., 2001; Wang et al., 2011), the value does not well represent  
827 observations in certain regions. Measurements by Shupe et al. (2001) and Leaitch et al.  
828 (2016) show an Arctic spring-summer-mean cloud liquid water content that is an order of  
829 magnitude lower ( $1 \times 10^{-7} \text{g cm}^{-3}$ ). During the spring and summer, more efficient aerosol  
830 removal in liquid clouds plays a key role in the control of aerosol distributions (Garrett et  
831 al., 2010). An overestimation of the liquid water content of Arctic clouds (by using a  
832 globally fixed value for  $L$ ) in our simulation would yield under-vigorous wet removal  
833 efficiency, particularly for cases of low intensity precipitation (low  $Q$ ). To address this  
834 issue, we replace the fixed value with the cloud liquid and ice water contents from the  
835 GEOS-5 assimilated meteorology fields and calculate the efficiency as the ratio of the  
836 grid-mean precipitation production rate and the grid-mean liquid and ice water  
837 contents. We impose a maximum efficiency ( $1 \times 10^{-3} \text{s}^{-1}$ ) to prevent over-vigorous

838 removal. This value is consistent with the upper limit for these process rates given in  
839 Gettelman et al. (2013).

840

841 In addition, we implement a temperature-dependent representation of the aerosol  
842 activated fraction (Verheggen et al., 2007) to account for the fraction of aerosol  
843 susceptible to wet removal in mixed-phase clouds. In mixed-phase clouds, only a fraction  
844 of the aerosols are contained in the cloud hydrometeors and susceptible to removal when  
845 cloud water and ice converts to precipitation. As clouds glaciate, cloud droplets evaporate  
846 and release aerosols from the condensed phase because ice crystals grow at the expense  
847 of cloud droplets due to differences in the saturation vapour pressure over liquid water  
848 and ice. The Verheggen et al. (2007) parameterization for activated fraction accounts for  
849 this effect, such that only a fraction of the total in-cloud aerosol is susceptible to wet  
850 removal as precipitation forms in mixed phase clouds. However, in strongly riming-  
851 dominated regimes, this may lead to an under-estimate of the removal.

852

853 We also develop the representation of the precipitation fraction. In the standard GEOS-  
854 Chem model, the fraction of the grid box that is precipitating,  $F$ , is

855

$$856 \quad F = Q / \beta L \quad \text{Eq. 2}$$

857

858 Replacing  $\beta$  with Eq. 1 and simplifying yields

859

$$860 \quad F = 1 / (1 + (k_{min} L / Q)) \quad \text{Eq. 3}$$

861

862 where  $k_{min}L$  has a fixed value of  $1 \times 10^{-10} \text{ g cm}^{-3} \text{ s}^{-1}$  in the standard model version. Thus,  
863 the precipitation fraction increases with precipitation production rate. We replace this  
864 parameterization by treating the precipitation fraction for aerosol scavenging in clouds as  
865 the cloud fraction from the GEOS-5 meteorological fields in the model layers where  
866 precipitation is produced. These wet scavenging developments were also implemented in  
867 a GEOS-Chem v9-03-01 simulation of  $^{137}\text{Cs}$  (also using GEOS5 met fields) and  
868 evaluated against  $^{137}\text{Cs}$  measurements taken for several weeks following the March 2011  
869 Fukushima Dai-Ichi nuclear power plant accident. Implementation of these scavenging  
870 revisions yielded improved agreement with the radionuclide measurements (median ratio  
871 of measured to modeled surface layer concentrations changed from 5.53 to 0.52) and  
872 reduced e-folding times from 21.8 days to 13.2 days, which is close to the measurement  
873 value of 14.3 days (Kristiansen et al., 2015). These wet removal revisions also slightly  
874 reduced the mean bias relative to measurements of the number of aerosols larger than 40  
875 nm (N40), 80 nm (N80) and 150 nm (N150) for the same global set of 21 geographically  
876 diverse sites as described in [D'Andrea et al. \(2013\)](#) (not shown).

877

878 Simulation NEWSCAV+COAG includes additional developments to the interstitial  
879 aerosol coagulation mechanism in clouds for the TOMAS microphysics scheme as  
880 explored in Pierce et al. (2015). This revised coagulation parameterization accounts for  
881 the order 100-fold increase in the wet size of aerosols that activate to form cloud  
882 droplets. This simulation assumes [for the purposes of coagulation only](#) that 1) aerosols  
883 that activate to form cloud droplets must have a dry diameter larger than 80 nm, 2) super-  
884 cooled clouds persist to temperatures as low as 238K and 3) all cloud droplets are 10  $\mu\text{m}$   
885 in diameter. While these are crude assumptions, they are within reasonable bounds and

886 allow examination of the potential of interstitial coagulation to control aerosol size  
887 distributions. The grid-box mean coagulation kernel between two size bins is calculated  
888 as

$$890 J_{i,j} = (1 - f_{cloudy}) K_{clear;i,j} N_i N_j + f_{cloudy} K_{cloudy;i,j} N_i N_j \quad \text{Eq. 4}$$

891

892 where  $J_{i,j}$  is the coagulation rate between particles in bins  $i$  and  $j$ ,  $f_{cloudy}$  is the fraction of  
893 the grid box that is cloudy,  $K_{clear}$  is the coagulation kernel between bins  $i$  and  $j$  in the clear  
894 portion of the gridbox,  $K_{cloudy}$  is the coagulation kernel between bins  $i$  and  $j$  in the cloudy  
895 portion of the gridbox,  $N_i$  is the number concentration of particles in bin  $i$ , and  $N_j$  is the  
896 number concentration of particles in bin  $j$ . While the activated particle is **treated as**  
897 **having** a diameter of 10  $\mu\text{m}$ , the unactivated collision-partner aerosol is **treated as having**  
898 a diameter following hygroscopic growth under grid-box mean relative humidity. If the  
899 in-cloud relative humidity is considerably greater than the grid mean, then the  
900 coagulation kernel could be overestimated. These developments to the interstitial aerosol  
901 coagulation parameterization in clouds are applied and evaluated in Pierce et al. (2015)  
902 and yielded improved agreement with in-situ aerosol size distributions at 21  
903 geographically diverse sites in the Northern Hemisphere.

904

905 Simulation NONUC turns off new particle formation (NPF) **globally** to examine the  
906 contribution of NPF to aerosol number in the Arctic. This simulation is otherwise  
907 identical to simulation NEWSCAV.

908

### 909 3. Observations and GEOS-Chem-TOMAS simulations of 910 **annual** cycles in Arctic aerosol number and size

911

#### 912 3.1 Observed **annual** cycle in Arctic aerosol number and size

913 Figure 1 shows the 2011-2013 monthly median aerosol number distributions from the  
914 SMPS at Alert and DMPS at Mt. Zeppelin. At both sites, the accumulation mode (defined  
915 here as particles with diameters from 0.1  $\mu\text{m}$  to 0.5  $\mu\text{m}$  due to instrument range, although  
916 typically extending to 1  $\mu\text{m}$ ) gradually builds during winter to a maximum in March and  
917 April. Afterward, the accumulation mode decreases while the Aitken mode (defined here  
918 as particles of 0.02  $\mu\text{m}$  to 0.1  $\mu\text{m}$  in diameter due to instrument range, although typically  
919 extending to 0.01  $\mu\text{m}$ ) increases in number to a maximum in July-August. October is  
920 characterized by the lowest number concentrations in both modes until the accumulation  
921 mode starts to build again in November. As a result, the total aerosol number at both  
922 locations has a shallow maximum in both spring and summer. In Fig. 1, the magnitude  
923 between the 20th to 80th percentiles for particles smaller than 100 nm is greatest during  
924 the months of June to August when NPF processes in the Arctic boundary layer are  
925 expected to make strong and episodic contributions to the aerosol number (e.g. Korhonen  
926 et al., 2008; Leaitch et al., 2013). The complete annual cycle is remarkably similar at both  
927 sites and similar to that observed at Mt. Zeppelin over an earlier ten-year period from  
928 2000 to 2010 (Fig. 7 in Tunved et al., 2013). The similarity in these number distributions  
929 across the one thousand km that separates Alert and Mt. Zeppelin suggests an annual  
930 cycle that spans the high Arctic. In the following sections we use the GEOS-Chem-  
931 TOMAS model to interpret the processes that control these cycles.

932

933 Figure 2 shows the **monthly median** aerosol effective diameter calculated **from the 2011-**  
934 **2013** measurements **with** SMPS at Alert, and DMPS at Mt. Zeppelin. The effective  
935 diameter is the ratio of the second and third moments of the aerosol number distribution,  
936 and is useful in determining the optical properties of an aerosol distribution, and for  
937 comparing between distributions. The effective diameter is defined as

938

$$939 \left| D_{\text{eff}} = \frac{\int_{D_{\text{min}}}^{D_{\text{max}}} D^3 N(D) dD}{\int_{D_{\text{min}}}^{D_{\text{max}}} D^2 N(D) dD} \quad \text{Eq. 5} \right.$$

940 where  $D$  is the aerosol diameter and  $N(D)$  is the aerosol number distribution. The integral  
941 here is taken over the **instrument** size range from  $D_{\text{min}} = 20$  nm to  $D_{\text{max}} = 500$  nm.

942 Despite the geographic distance of these two sites, the **annual** cycle of the aerosol  
943 effective diameter is remarkably similar. At both sites, the aerosol effective diameter  
944 shows a strong **annual** cycle with a minimum during the summer months of about 180 nm  
945 and a maximum in the winter of about 260 nm. The effective diameter at Mt. Zeppelin  
946 exceeds Alert by about 10-20% throughout the year. In the next sections, we interpret  
947 these observed **annual** cycles in number and size using the GEOS-Chem-TOMAS model.  
948

### 949 **3.2. Interpreting processes controlling the annual cycle of** 950 **aerosol number and size with GEOS-Chem-TOMAS**

951

952 Figures 3 and 4 show the seasonal-median number distributions **from measurements at**  
953 **Alert and Mt. Zeppelin, respectively, for winter (DJF), spring (MAM), summer (JJA),**  
954 **and fall (SON), and also for our four simulations. The measurement distributions exhibit**

955 the key features of Arctic aerosol size distributions, a dominant Aitken mode in summer,  
956 a dominant accumulation mode with suppressed Aitken mode in non-summer seasons,  
957 and minimum number in fall. To assist in interpreting Figs. 3 and 4, we calculate the  
958 fractional bias between the observed and simulated total number of aerosols over two size  
959 ranges available from the measurement data: 1) Aitken particles 20-100 nm in diameter  
960 and 2) accumulation particles 100-500 nm in diameter. We apply a size limit of 20-500  
961 nm to the Mt. Zeppelin measurement data and to our simulations to be consistent with the  
962 available data from Alert. We define fractional bias (*FB*) as

$$963 \quad FB = (C_m - C_o)/C_o \quad \text{Eq. 6}$$

964 where  $C_m$  is the model value and  $C_o$  is the observed value. These seasonal fractional bias  
965 values are presented in Tables 2 and 3. Among all four simulations, simulation STD  
966 never has the fractional bias closest to zero for the size ranges considered in Tables 2 and  
967 3.

968

969 The strong control of wet removal on Arctic aerosol number and size distributions  
970 throughout the annual cycle is highlighted by comparison of simulations STD and  
971 NEWSCAV in Figs. 3 and 4 and in Tables 2 and 3. For both Alert and Mt. Zeppelin, the  
972 standard GEOS-Chem-TOMAS model (simulation STD) overestimates the observed  
973 number of 100-500 nm diameter particles in all seasons as quantified by the positive  
974 fractional bias values in Tables 2 and 3. At both Alert and Mt. Zeppelin, this bias is  
975 reduced in spring and summer for simulation NEWSCAV relative to STD. The bias  
976 reduction is greatest in summer when aerosol wet removal by precipitation is more  
977 efficient within the Arctic boundary layer, and strongly limits the accumulation-mode

978 number at the surface sites. The efficiency of wet removal is parameterized to increase  
979 with temperature (from 238 K to 273 K) in our simulations. In seasons other than  
980 summer, wet removal in the Arctic boundary layer is less efficient. However, wet  
981 removal outside the Arctic boundary layer continues to influence the number of  
982 accumulation-mode particles transported to the measurement sites. Over a limited size  
983 range (200-500 nm diameter particles) and in all seasons at both sites, NEWSCAV is a  
984 closer match to measurements than STD, but the difference between STD and  
985 NEWSCAV is very small at Alert in winter and spring.

986

987 Wet removal also has feedbacks that particularly influence Aitken-mode and 100-200 nm  
988 diameter particle numbers indirectly through changes in NPF and subsequent particle  
989 growth to these sizes. Figures 3 and 4 show that at both sites and in all seasons, more  
990 vigorous wet removal in simulation NEWSCAV relative to STD yields more numerous  
991 Aitken-mode particles (although the springtime difference is very small), and in fall and  
992 winter, also more numerous 100-200 nm particles. A reduction in surface area of 200-500  
993 nm aerosols by more vigorous wet removal (simulation NEWSCAV relative to STD)  
994 promotes NPF and particle growth. Other than in summer, this NPF occurs primarily  
995 outside the Arctic boundary layer and growth occurs during transport to the measurement  
996 sites. As a result of the increase in number of 20-200 nm particles in simulation  
997 NEWSCAV relative to STD, the accumulation-mode bias is greater for NEWSCAV in  
998 fall and winter at both sites and the Aitken mode bias is greater for NEWSCAV in fall,  
999 winter and spring at both sites (Tables 2 and 3).

1000

1001 The balance of these processes of NPF, growth, and wet removal is a challenge for Arctic  
1002 simulations of number and size. In all seasons at both sites (except for summer at Mt.  
1003 Zeppelin), NEWSIM strongly over estimates the number of 20-40 nm diameter  
1004 particles. Nonetheless, among the four simulations NEWSIM has the closest-to-zero  
1005 bias for the 20-100 nm and 100-500 nm diameter particles at Mt. Zeppelin in summer. As  
1006 well, at Alert, the summertime Aitken-mode bias for simulation NEWSIM is second  
1007 smallest (after NEWSIM+COAG), but the shape of the distribution shown in Fig. 3 is  
1008 not a perfect match with the observations for either simulation as there are sizes that are  
1009 strongly over- and under-predicted within the 20-100 nm diameter range.

1010

1011 Figures 3 and 4 demonstrate the importance of in-cloud coagulation  
1012 (NEWSIM+COAG relative to NEWSIM) in reducing the number of 20-200 nm  
1013 diameter particles in all seasons but to varying degrees. In spring and summer at both  
1014 sites, this additional coagulation for simulation NEWSIM+COAG reduces the number  
1015 of 40-100 nm diameter particles excessively relative to measurements. As a result,  
1016 simulation NEWSIM is a somewhat better match to measurements in this 40-100 nm  
1017 diameter range in spring and summer at both sites. However among the four simulations,  
1018 NEWSIM+COAG has the smallest fractional bias for the Aitken mode in winter and  
1019 summer at Alert, and in winter and spring at Mt. Zeppelin, as well as the smallest  
1020 springtime accumulation-mode bias at both sites (and smallest summertime  
1021 accumulation-mode bias at Alert).

1022

1023 Simulation NONUC was designed as a means to assess the relative contribution of NPF  
1024 processes to the Arctic aerosol size distributions. In our simulations, NPF contributes

1025 most strongly to the number of particles smaller than 200 nm. These contributions occur  
1026 in all seasons as shown by the differences between NEWSVAC and NONUC in Figs. 3  
1027 and 4. In the summertime, NPF occurs within the Arctic boundary layer both in our  
1028 simulations and in observations (Chang et al, 2011; Leaitch et al., 2013; Allan et al.,  
1029 2015; Croft et al., submitted). At this time of year, the Arctic region has greater  
1030 production of oxidants such as OH and has greater dimethyl sulphide (DMS) emissions  
1031 from the oceanic biological activity, such that oxidation of DMS by OH produces sulphur  
1032 dioxide (SO<sub>2</sub>) and ultimately, sulphuric acid, which contributes to particle formation  
1033 processes in the boundary layer (e.g. Leaitch et al., 2013). In seasons other than summer,  
1034 transport of particles arising from NPF outside the Arctic or NPF above the Arctic  
1035 boundary layer contribute more to the number of particles with diameters smaller than  
1036 200 nm. The NONUC simulation coincidentally has lowest bias for the accumulation-  
1037 mode number in fall and winter at both sites, and for the Aitken mode in fall at both sites,  
1038 as well as in spring at Alert. Shutting off the NPF process (a source term) in the model  
1039 appears to compensate for errors in the key sink terms for aerosol number, such as wet  
1040 removal and coagulation, and related feedbacks. In reality, NPF makes a significant  
1041 contribution to the number concentration in the Arctic (e.g. Chang et al., 2011; Leaitch et  
1042 al., 2013). The Arctic is a challenging region that tests the performance of the entire set of  
1043 model mechanisms. Nevertheless, our results, presented in Figs. 3 and 4, highlight NPF  
1044 and particle growth, wet removal, and coagulation as key processes for controlling Arctic  
1045 aerosol size distributions throughout the annual cycle.  
1046

1047 Figures 5 and 6 show the annual cycle of the monthly median total number of particles  
1048 with diameters between 20-500 nm (N20), 80-500 nm (N80), and 200-500 nm (N200)  
1049 from simulations and from measurements at Alert and Mt. Zeppelin. To assist with  
1050 interpreting Figs. 5 and 6, Tables 4 and 5 contain the mean fractional bias (MFB) and  
1051 mean fractional error (MFE) following Boylan and Russell (2006).

$$MFB = \frac{1}{N} \sum_{i=1}^{i=N} \frac{(C_m(i) - C_o(i))}{(C_m(i) + C_o(i))/2}$$

1052 Eq. 7

$$MFE = \frac{1}{N} \sum_{i=1}^{i=N} \frac{|C_m(i) - C_o(i)|}{(C_m(i) + C_o(i))/2}$$

1053 Eq. (8)

1054 where  $C_m(i)$  is the  $i^{\text{th}}$  monthly model value,  $C_o(i)$  is the  $i^{\text{th}}$  monthly measurement value  
1055 and  $N$  is the total number of months in a year.

1056

1057 Figures 5 and 6 demonstrate the key features of the annual cycle of integrated Arctic  
1058 aerosol number distributions. Measurements from both Alert and Mt. Zeppelin show a  
1059 shallow maximum in the N20 in both spring and summer. The measurement N80 and  
1060 N200 have a maximum in March-April at both sites. The minimum for the N20, N80 and  
1061 N200 from measurements occurs near September-October at both sites. All four  
1062 simulations capture the general trend of N80 and N200 being higher in spring than in fall,  
1063 but there are some notable mismatches discussed below.

1064

1065 Similar to our findings in examining the seasonal-mean size distributions (Figs 3 and 4),  
1066 Figs. 5 and 6 show that the N200 is highly sensitive to the wet removal parameterization.  
1067 Simulation STD over-predicts the N200 at both Alert and Zeppelin as evidenced by the  
1068 greatest magnitude of the N200 MFB and MFE among the four simulations at both sites  
1069 for simulation STD. Wet removal revisions for simulation NEWSCAV reduce the N200  
1070 MFB and MFE towards zero, whereas implementation of the new coagulation mechanism  
1071 has a lesser effect on these N200 biases. NONUC has the closest-to-zero MFB for N200  
1072 among the four simulations at both Alert and Zeppelin and also the lowest MFE at Alert.  
1073 However, the MFE for the N200 is similar between NONUC and NEWSCAV+COAG at  
1074 both sites. As noted earlier, suppressing particle formation in NONUC likely  
1075 compensates for errors in sink processes.

1076

1077 The N20 and N80 are sensitive to the wet removal and coagulation schemes. Tables 4 and  
1078 5 show that interstitial coagulation (NEWSCAV+COAG relative to NEWSCAV) reduces  
1079 the MFB and MFE, for N20 and N80 at both Alert and Mt. Zeppelin. However, changes  
1080 to the wet-removal parameterization increase the N20 and N80 MFB and MFE at both  
1081 sites for simulation NEWSCAV relative to STD, except for the N80 MFB at Mt.  
1082 Zeppelin. As discussed in reference to Figs. 3 and 4, NPF increases when the wet  
1083 removal is more vigorous, and these new particles grow to increase the number of  
1084 Aitken-mode aerosols in the simulations (i.e. the condensation sink for condensable  
1085 vapours on to existing aerosols is lower, which favours NPF and growth and reduces  
1086 losses of new particles by coagulation). At Mt. Zeppelin for the N20 and N80, NONUC  
1087 has the smallest MFB but NEWSCAV+COAG best represents the annual cycle (smallest

1088 MFE) among the four simulations. At Alert, for the N20 and N80, NEWSCAV+COAG  
1089 best represents the annual cycle (smallest MFE and MFB).  
1090  
1091 Figures 5 and 6 also show the annual cycle of aerosol effective diameter at both Alert and  
1092 Mt. Zeppelin for our simulations and from measurements. The simulation  
1093 NEWSCAV+COAG has the closest agreement (smallest MFE) with the annual cycle of  
1094 effective diameter from the measurements for both sites. At Alert, the aerosol effective  
1095 diameter has the smallest bias for both NEWSCAV and NEWSCAV+COAG, whereas, at  
1096 Mt. Zeppelin, STD has the smallest bias for the effective diameter due to cancellation of  
1097 errors between months of over- and under-prediction. The simulations over-predict the  
1098 aerosol effective diameter in July and August, except for NEWSCAV at Mt. Zeppelin.  
1099 The over-prediction of summertime effective diameter is pronounced for the simulation  
1100 NONUC that removes NPF, illustrating the importance of NPF in yielding the  
1101 summertime minimum effective diameter. The effective diameter in winter at Mt.  
1102 Zeppelin is strongly underestimated in all simulations, reflecting too many small (Aitken  
1103 mode) particles, even for simulation NONUC.  
1104  
1105 The similarity in the annual cycle of effective diameter from measurements at both Alert  
1106 and Zeppelin suggests a cycle that occurs throughout the Arctic. Figure 7 shows the  
1107 seasonal-mean pan-Arctic geographic distribution of the surface layer effective diameter  
1108 for the NEWSCAV+COAG simulation. Throughout the Arctic, the simulated effective  
1109 diameter declines to a minimum in summer. In Fig. 7, we superimpose the effective  
1110 diameter from observations at Alert and Mt. Zeppelin. The simulated effective diameter

1111 at the altitude of Mt Zeppelin (500 m) is smaller than the surface value shown here (by 35  
1112 nm in summer, 20 nm in fall and 5 nm in winter and spring).

1113

### 1114 **3.3. Process rates controlling the *annual* cycle in Arctic aerosol** 1115 ***number and size***

1116

1117 Figure 8 shows the monthly- and regional-mean process rates that control aerosol number  
1118 in four size ranges for the entire troposphere north of the Arctic Circle (66 °N) for  
1119 simulation NEWSCAV+COAG. Source processes for aerosol number are positive and  
1120 sink processes are negative.

1121

1122 The number of aerosols smaller than 10 nm in diameter (nucleation-mode size) is  
1123 primarily controlled by NPF (particle formation, also termed nucleation), coagulation,  
1124 and transport. There are two maxima in the particle formation rate shown in Fig. 8 (top-  
1125 left panel), one in early spring (March) and one in summer (July). In spring, simulated  
1126 NPF occurs mainly in the free troposphere, whereas in summer, NPF occurs also in the  
1127 boundary layer. In the summertime Arctic boundary layer, NPF is enhanced by the low  
1128 aerosol surface area due to efficient wet removal of accumulation-mode aerosols by  
1129 episodic rain and summer enhancements in sulphuric acid production rates (from  
1130 oxidation of DMS). The simulated early-spring NPF rate maximum for nucleation-size  
1131 particles is associated with NPF in the middle and upper troposphere, and as a result is  
1132 not evident in the measurements at Alert and Mt. Zeppelin. This simulated springtime  
1133 maximum in NPF occurs because the precursors for sulphuric acid (DMS, SO<sub>2</sub>) are

1134 transported from open ocean areas and pollution sources at lower latitudes. Then NPF  
1135 proceeds in locations where the condensation sink for sulphuric acid on existing aerosols  
1136 is low such as following wet scavenging episodes.

1137

1138 The top-left panel of Fig. 8 shows that transport reaches a maximum during winter, while  
1139 NPF reaches a minimum such that the two are comparable sources for the entire Arctic  
1140 troposphere. Simulated NPF occurs in the dark Arctic wintertime since the oxidant OH is  
1141 produced through reaction of ozone and volatile organic compounds, although the OH  
1142 mixing ratios are three-fold less than in summer. As a result, sulphuric acid (a particle  
1143 precursor vapour) can be produced through oxidation by OH of DMS and sulphur dioxide  
1144 ( $\text{SO}_2$ ) transported into the Arctic in winter. Our simulated Arctic wintertime sulphuric  
1145 acid mixing ratio is about 0.01 ppt near the tropopause and diminishes towards the  
1146 Earth's surface. Measurements by Möhler and Arnold (1992) indicate wintertime  
1147 sulphuric acid levels in Northern Scandinavia of about 0.1 ppt near the tropopause  
1148 decreasing to 0.01 ppt near the Earth's surface, implying the true nucleation rate could be  
1149 even higher.

1150

1151 Figure 9 shows aerosol number transport rates at different altitudes by decomposing the  
1152 rates from Fig. 8 into four altitude bands. Nucleation-mode particles are mostly  
1153 transported in the mid to upper troposphere (at altitudes between 4 and 10 km) where the  
1154 coagulation sink is sufficiently low that nucleation-mode particles can persist. At these  
1155 altitudes and particularly when the atmosphere just been cleaned by a precipitation event,  
1156 if the Aitken- and accumulation-mode concentrations are low ( $5\text{-}10\text{ cm}^{-3}$ ), then  
1157 nucleation-mode particles can have a lifetime of about one week with respect to loss by

1158 coagulation. Transport rates for nucleation size-particles are greatest from January to  
1159 March.  
1160  
1161 Figure 8 (top-right panel) indicates that several processes control the simulated Aitken-  
1162 mode number in the Arctic troposphere. Northward transport is the dominant source  
1163 process for the Arctic Aitken mode during all months of the year. This transport of  
1164 simulated Aitken-mode aerosols occurs throughout the troposphere as shown in Fig. 9.  
1165 Figure 8 shows that during the Arctic spring (March-April), when the total aerosol mass  
1166 is greatest, condensational growth of existing aerosols makes a relatively greater  
1167 contribution to the total source rates for Aitken-mode particles. This net enhancement in  
1168 condensational growth includes condensational loss of Aitken-mode particles to  
1169 accumulation-mode sizes such that the nucleation mode is a larger source of Aitken-mode  
1170 particles than apparent in the figure. Simulated primary particle emissions within the  
1171 Arctic have a relatively constant source rate for the Aitken mode throughout the year,  
1172 quite similar in magnitude to the maximum condensational growth rate in March-April.  
1173 Coagulation is the dominant sink for the Aitken mode with dry deposition accounting for  
1174 the majority of the remaining sink. Simulated removal of the Aitken- mode number by  
1175 wet deposition is a weaker sink than dry deposition because the smaller Aitken-mode  
1176 aerosols have inefficient removal by activation scavenging (the process of aerosols acting  
1177 as the seed for cloud-droplet and ice-crystal formation and subsequent removal during  
1178 precipitation). Recent studies indicate that aerosols as small as 50 nm - 60 nm can  
1179 activate in the clean Arctic summertime conditions (Leaith et al., 2013; Leaith et al.,  
1180 2016) and we likely under-estimate this removal in our simulations. Figure 8 does show  
1181 an increase in wet removal as a sink for the Aitken mode in summer as this process

1182 becomes more efficient at warmer temperatures and aerosols larger than about 60 nm are  
1183 removed by activation scavenging in our simulations.

1184

1185 For the accumulation-mode particle number simulation, Fig. 8 (bottom-left panel)  
1186 indicates that the dominant sources are northward transport and condensational growth,  
1187 which also includes production of sulphate by in-cloud oxidation. These two simulated  
1188 source terms are roughly equal in magnitude in the Arctic throughout April to October.

1189 Northward transport of accumulation-mode aerosols persists in the simulation in all  
1190 seasons, with a minimum in winter and an increase in March-April. Figure 9 shows that  
1191 transport of accumulation size aerosol at altitudes between 1.5 km and 4 km reaches a  
1192 maximum in April, which would contribute to the well-known Arctic haze phenomena.

1193 Figure 9 also shows that the majority of simulated accumulation-mode number transport  
1194 is below 1.5 km. This low-level transport is persistent though diminished throughout the  
1195 summer; suggesting that the summertime cleanliness of the Arctic near-surface  
1196 atmosphere relies heavily on the increased efficiency of the removal processes in the  
1197 lower troposphere during the summer months. Indeed, Fig. 8 shows that wet removal is  
1198 the dominant accumulation aerosol number sink process in all seasons, but increases in  
1199 magnitude and relative importance with respect to dry deposition in the summer,  
1200 accounting for about 90% of the total summertime sink rate. In winter, the relative  
1201 simulated importance of dry deposition for accumulation aerosol number increases,  
1202 although remains below 25% of the total sink rate.

1203

1204 Since wet removal has large effects on the accumulation aerosol number associated with  
1205 Arctic springtime pollution, we further examined its annual cycle. Figure 10 shows the

1206 monthly- and regional-mean accumulation-mode number lifetime with respect to wet  
1207 removal for layers of the lower troposphere. Longer lifetimes from December to March  
1208 contribute to the build up of the Arctic haze layer, particularly as this is combined with  
1209 transport of pollution into the Arctic during wintertime. The spring to summer transition  
1210 period is characterized by a rapid increase in the efficiency of wet scavenging that  
1211 contributes to removal of the Arctic haze in April-May. Figure 10 shows about a 5-fold  
1212 decrease in wet removal lifetime in the Arctic 1.5-4 km layer from February to April.  
1213 Simulated wet removal lifetimes in the Arctic boundary layer below 1.5 km reach a  
1214 minimum in October, such that when combined with diminishing new particle formation  
1215 as the sunsets and limited transport yields the simulated total aerosol number minimum in  
1216 the fall season, similar to that observed at Alert and Mt. Zeppelin. To put the Arctic  
1217 region in context, Fig. 10 also shows the lifetimes with respect to wet removal for the  
1218 region north of 50°N, indicating that wet removal processes are generally more efficient  
1219 for a region with greater southward extent and at lower altitudes.

1220

1221 Figure 8 shows that the simulated coarse mode is controlled primarily by emissions,  
1222 transport and wet deposition. In early spring (March-April), northward transport of  
1223 coarse-mode aerosols (dust and sea-salt emissions) is not quite matched by the removal  
1224 processes. The resultant residual (black line on Fig. 8) gives the net rate of either aerosol  
1225 build-up or loss for the regional monthly mean number. In early spring, there is a net  
1226 build-up of coarse-mode aerosol in the Arctic region. However as spring progresses, there  
1227 is a net loss such that the net residual integrates to zero over the annual cycle. Wet  
1228 removal is the primary loss process in all seasons in this simulation. Figure 9 shows that

1229 the early springtime transport of the coarse mode occurs mainly at altitudes between 1.5  
1230 and 4 km, a time when the polar dome still extends relatively far southward.

1231

1232 In this section we examined process rates over the entire troposphere north of 66 °N. To  
1233 put these Arctic process rates in context with other regions, Fig. 11 shows the same set of  
1234 processes for the same four aerosol size ranges over the entire troposphere north of  
1235 50 °N. Several differences are apparent. For the nucleation, Aitken and accumulation  
1236 sizes, transport is of negligible importance relative to other source processes, unlike for  
1237 the Arctic region. Coagulation remains the main sink for the number of nucleation- and  
1238 Aitken-mode aerosols as shown in Figs. 8 and 11, but the relative importance of wet  
1239 removal of the Aitken mode in summer has diminished. Wet removal rates for the  
1240 accumulation-mode aerosol number reach a maximum in May in the Arctic whereas the  
1241 maximum is in July for the entire region north of 50°N. For the Aitken and accumulation  
1242 modes, condensational growth is the dominant source north of 50 °N, unlike for the  
1243 Arctic region only (Fig. 8) where transport was of similar or greater importance. The  
1244 coarse mode north of 50 °N shows a peak in the transport source in April, similar to Fig.  
1245 8, associated with transport of dust from lower latitudes in spring. Coarse-particle number  
1246 wet removal also shows an April maximum in both Figs. 8 and 11. The global mean  
1247 simulated number process rates (not shown) show a relative importance of processes  
1248 similar to that in Fig.11, except in the global mean, primary emissions are the only non-  
1249 negligible source of coarse aerosol number throughout the year. Wet deposition remains  
1250 the dominant sink of accumulation and coarse-mode number, followed by dry deposition  
1251 at the global scale, as in the Arctic.

1252

## 1253 **4. Conclusions**

1254 In this study, we examined the annual cycle of aerosol number and size distributions in  
1255 the Arctic from measurements made during 2011-2013 by scanning mobility particle  
1256 sizer (SMPS) at Alert and by differential mobility particle sizer (DMPS) at Mt. Zeppelin.  
1257 There was a strong and similar annual cycle in measurements of aerosol number and size  
1258 at both sites despite their geographic separation of 1000 km. The annual cycle in the total  
1259 number of aerosols larger than 20 nm had two maxima. The maximum in spring was  
1260 dominated by accumulation-mode aerosols (particles 100 nm to 500 nm in diameter) and  
1261 in summer was dominated by Aitken-mode aerosols (particles 20 nm to 100 nm in  
1262 diameter). At both sites, total aerosol number reached a minimum in October. The annual  
1263 cycle of aerosol effective diameter derived from measurements had an inter-seasonal  
1264 range between 180 nm and 260 nm, with a minimum in the summer. These annual  
1265 cycles were similar to those presented by Tunved et al. (2013) based on earlier data at Mt.  
1266 Zeppelin between the years 2000 and 2010.

1267

1268 We interpreted these annual cycles in Arctic aerosol number and size with the GEOS-  
1269 Chem-TOMAS aerosol microphysics model. Our simulations indicated a strong  
1270 sensitivity of the annual cycle of Arctic aerosol number and size to several key processes;  
1271 new-particle formation (NPF), interstitial coagulation scavenging in clouds, wet removal  
1272 through precipitation, and transport.

1273

1274 Our GEOS-Chem-TOMAS simulations demonstrated that wet removal had a strong  
1275 control on Arctic aerosol number distributions throughout the annual cycle, similar to the  
1276 findings of earlier studies focused on spring-summer (Korhonen et al, 2008) and Arctic  
1277 aerosol mass abundance (e.g. Garrett et al., 2010; Browse et al., 2012; Sharma et al.,  
1278 2013). In our study, wet removal updates were developed for the GEOS-Chem-TOMAS  
1279 model that together increased the efficiency of wet removal. We replaced the global-  
1280 constant cloud liquid water content with the values from GEOS-5 assimilated  
1281 meteorology fields, updated the gridbox precipitation fraction, and implemented the  
1282 Verheggen et al. (2007) temperature-dependent aerosol activation fraction to account for  
1283 the fraction of aerosol assumed to be susceptible to wet removal in mixed-phase clouds.  
1284 In our updated-removal simulation, efficient wet removal in the Arctic summertime  
1285 boundary layer strongly limited the accumulation-mode number despite an ongoing  
1286 source through transport and condensational growth. The wet removal updates reduced  
1287 model-measurement bias (relative to the standard model) for the number of aerosols  
1288 larger than 200 nm in all seasons at both Alert and Mt. Zeppelin (although the changes in  
1289 winter and spring at Alert were relatively small).

1290

1291 More vigorous wet removal promoted NPF and growth in our simulations and  
1292 contributed to a summertime dominant Aitken mode since a reduction in the surface area  
1293 of accumulation size aerosols (the condensation sink for sulphuric acid) influences the  
1294 likelihood that sulphuric acid will participate in NPF as opposed to condensing on  
1295 existing aerosols. Indeed, the more vigorous wet removal scheme increased the simulated  
1296 Aitken-mode number in all seasons at Alert and Mt. Zeppelin (although the springtime

1297 Aitken mode was relatively less sensitive to the changes made in our study). Outside of  
1298 summer, NPF and growth occurred mostly outside the Arctic boundary layer. A  
1299 sensitivity study with no NPF globally indicated that NPF strongly controls the number  
1300 of particles with diameters smaller than 200 nm in all seasons in the Arctic, while  
1301 particularly important in yielding the summertime Aitken-mode dominance.

1302

1303 From February to April, the simulated accumulation-mode wet removal efficiency at  
1304 altitudes of the springtime Arctic haze layer (between 1.5 and 4 km) increased by 5-fold,  
1305 contributing to our simulation of the spring-summer transition from Aitken- to  
1306 accumulated-mode dominated Arctic size distributions (e.g. Engvall et al., 2008;  
1307 Korhonen et al., 2008). In the boundary layer, simulated wet removal efficiency reached a  
1308 maximum (lowest accumulation-mode aerosol number lifetime) in October. The observed  
1309 total aerosol number minimum in October was reproduced in our simulations due to  
1310 efficient wet removal combined with diminished boundary layer NPF due to lower  
1311 sulphuric acid concentrations and limited transport.

1312

1313 We also found an important role for coagulation of interstitial aerosols in clouds with  
1314 aerosols of larger size that have activated to form cloud droplets. There has been  
1315 relatively less attention given to the importance of this process in controlling Arctic size  
1316 distributions despite the Arctic being a region with widespread cloud cover in all seasons.  
1317 Implementation of an interstitial coagulation mechanism in clouds in our simulations  
1318 reduced the number of aerosols with diameters smaller than 200 nm in all seasons at both  
1319 Alert and Mt. Zeppelin. In some seasons this reduction in the Aitken-mode number  
1320 worsened model-measurement agreement, highlighting the delicate balance between the

1321 processes of coagulation, NPF, growth and wet removal in control of the Arctic size  
1322 distributions that is challenging to simulate. Our simulations tended to under predict the  
1323 number of larger Aitken-mode aerosols (40-100 nm in diameter) in summer and this is  
1324 the subject of ongoing investigation related to aerosol sources and growth.

1325

1326 The high sensitivity of aerosol number to interstitial coagulation in clouds suggests that  
1327 size-resolved models should include this process. However, many present-day global  
1328 models neglect this process, including previous versions of GEOS-Chem-TOMAS  
1329 (D'Andrea et al., 2013; Pierce et al., 2013; Trivitayanurak et al., 2008), GISS-TOMAS  
1330 (Adams and Seinfeld, 2002; Pierce and Adams, 2009), GLOMAP (Spracklen et al.,  
1331 2005a,b; 2008, Mann et al., 2012), GLOMAP-Mode (Mann et al., 2010; 2012, Lee et al.,  
1332 2013b), GEOS-Chem-APM (Yu and Luo, 2009; Yu, 2011) and IMPACT (Herzog et al.,  
1333 2004; Wang and Penner, 2009). To our knowledge, only a few models such as MIRAGE  
1334 and ECHAM-HAM (Herzog et al., 2004; Ghan et al., 2006; Hoose et al., 2008) represent  
1335 this process.

1336

1337 Our results highlight the importance of aerosol processes (as well as their delicate balance  
1338 and interactions) that continue to be poorly understood; 1) new-particle formation (NPF)  
1339 and growth, 2) in-cloud interstitial coagulation, and 3) wet removal as playing a key role  
1340 in the control of the annual cycle of aerosol number and size in the Arctic. The relative  
1341 importance of the processes that control aerosol number could change in a future  
1342 warming Arctic climate and also as emissions within the Arctic change.

1343

1344

1345 **Acknowledgements:**

1346 The authors acknowledge the financial support provided for NETCARE through the  
1347 Climate Change and Atmospheric Research Program at NSERC Canada. Thanks to  
1348 Sangeeta Sharma, Desiree Toom, Andrew Platt and the Alert operators for supporting the  
1349 Alert observations. We are also grateful to Ilona Riipinen, Jan Julin and Tinya Olenius for  
1350 helpful discussions and for providing the Atmospheric Cluster Dynamics Code (ACDC),  
1351 applied in our GEOS-Chem-TOMAS simulations.

1352  
1353 **References:**

1354  
1355  
1356 Adams, P. J. and Seinfeld, J. H.: Predicting global aerosol size distributions in general  
1357 circulation models, *J. Geophys. Res.*, 107(D19), 4310–4370, 2002.  
1358  
1359 Adams, P. J. and Seinfeld, J. H.: Disproportionate impact of particulate emissions on  
1360 global cloud condensation nuclei concentrations, *Geophys. Res. Lett.*, 30(5), 1210–1239,  
1361 2003.  
1362  
1363 Albrecht, B. A.: Aerosols, Cloud Microphysics, and Fractional Cloudiness, *Science*,  
1364 245(4923), 1227–1230, 1989.  
1365  
1366 Baranizadeh, E., Murphy, B. N., Julin, J., Falahat, S., Reddington, C. L., Arola, A.,  
1367 Mikkonen, S., Fountoukis, C., Patoulias, D., Minikin, A., Hamburger, T., Laaksonen, A.,  
1368 Pandis, S. N., Vehkamäki, H., Lehtinen, K. E. J. and Riipinen, I.: Implementation of  
1369 state-of-the-art ternary new particle formation scheme to the regional chemical transport

1370 model PMCAMx-UF in Europe, *Geosci. Model. Dev. Discuss.*, doi:10.5194/gmd-2016-  
1371 21, 2016.

1372

1373 Bey, I., Jacob, D. J., Yantosca, R. M., Logan, J. A., Field, B. D., Fiore, A. M., Li, Q., Liu,  
1374 H. Y., Mickley, L. J. and Schultz, M. G.: Global modeling of tropospheric chemistry with  
1375 assimilated meteorology: Model description and evaluation, *J. Geophys. Res.*, 106(D19),  
1376 23073, doi:10.1029/2001JD000807, 2001.

1377

1378 Boylan, J. W. and Russell, A. G.: PM and light extinction model performance metrics,  
1379 goals, and criteria for three-dimensional air quality models, *Atmos. Environ.*, 40, 4946-  
1380 4959, 2006.

1381

1382 Breider, T. J., Mickley, L. J., Jacob, D. J., Ge, C., Wang, J., Payer, M., Wang, Q., Fisher,  
1383 J., Ridley, D., McConnell, J., Sharma, S., et al.: 1980-2010 changes in Arctic Radiative  
1384 Forcing from Aerosols (in prep).

1385

1386 Browse, J., Carslaw, K. S., Arnold, S. R., Pringle, K. and Boucher, O.: The scavenging  
1387 processes controlling the seasonal cycle in Arctic sulphate and black carbon aerosol,  
1388 *Atmos. Chem. Phys.*, 12(15), 6775–6798, doi:10.5194/acp-12-6775-2012, 2012.

1389

1390 Browse, J., Carslaw, K. S., Mann, G. W., Birch, C. E., Arnold, S. R. and Leck, C.: The  
1391 complex response of Arctic aerosol to sea-ice retreat, *Atmos. Chem. Phys.*, 14(14), 7543–  
1392 7557, doi:10.5194/acp-14-7543-2014, 2014.

1393

1394 Cesana, G., Kay, J. E., Chepfer, H., English, J. M. and de Boer, G.: Ubiquitous low-level  
1395 liquid-containing Arctic clouds: New observations and climate model constraints from  
1396 CALIPSO-GOCCP, *Geophys. Res. Lett.*, 39(20), n/a–n/a, doi:10.1029/2012GL053385,  
1397 2012.  
1398  
1399 Chang, R. Y.-W., Leck, C., Graus, M., Müller, M., Paatero, J., Burkhardt, J. F., Stohl, A.,  
1400 Orr, L. H., Hayden, K., Li, S.-M., Hansel, A., Tjernström, M., Leaitch, W. R. and Abbatt,  
1401 J. P. D.: Aerosol composition and sources in the central Arctic Ocean during ASCOS,  
1402 *Atmos. Chem. Phys.*, 11, 10619-10636, doi:10.5194/acp-11-10619-2011, 2011.  
1403  
1404 Charlson, R. J., Schwartz, S. E., Hales, J. M., Cess, R. D., Coakley, J. A., Hansen, J. E.  
1405 and Hofman, D. J.: Climate Forcing by Anthropogenic Aerosols, *Science.*, 255(5043),  
1406 423–430, 1992.  
1407  
1408 Croft, B., Wentworth, G., Leaitch, W. R., Kodros, J., Murphy, J. G., Abbatt, J. P. D.,  
1409 Martin, R. V., and Pierce, J. R.: Contribution of Arctic seabird ammonia to atmospheric  
1410 particles and cloud radiative effect, *Nature Geosci.* (submitted).  
1411  
1412 D'Andrea, S. D., Hakkinen, S. A. K., Westervelt, D. M., Kuang, C., Levin, E. J. T.,  
1413 Kanawade, V. P., Leaitch, W. R., Spracklen, D. V., Riipinen, I., and Pierce, J. R.:  
1414 Understanding global secondary organic aerosol amount and size-resolved  
1415 condensational behavior, *Atmos. Chem. Phys.*, 13, 11519-11534, doi:10.5194/acp-13-  
1416 11519-11534, 2013.  
1417

1418 Di Pierro, M., Jaeglé, L., Eloranta, E. W. and Sharma, S.: Spatial and seasonal  
1419 distribution of Arctic aerosols observed by the CALIOP satellite instrument (2006–2012),  
1420 *Atmos. Chem. Phys.*, 13(14), 7075–7095, doi:10.5194/acp-13-7075-2013, 2013.  
1421  
1422 Donahue, N. M., Trump, E. R., Pierce, J. R., and Riipinen, I.: Theoretical constraints on  
1423 pure vapour-pressure driven condensation of organics to ultrafine particles, *Geophys.*  
1424 *Res. Lett.*, 38, L16801, doi:10.1029/2011GL048115, 2011.  
1425  
1426 Engvall, A. C., Krejci, R., Ström, J., Minikin, A., Treffeisen, R., Stohl, A. and Herber, A.:  
1427 In-situ airborne observations of the microphysical properties of the Arctic tropospheric  
1428 aerosol during late spring and summer, *Tellus, Ser. B Chem. Phys. Meteorol.*, 60 B(3),  
1429 392–404, doi:10.1111/j.1600-0889.2008.00348.x, 2008.  
1430  
1431 Fu, P. Q., Kawamura, K., Chen, J., Charrière, B. and Sempéré, R.: Organic molecular  
1432 composition of marine aerosols over the Arctic Ocean in summer: Contributions of  
1433 primary emission and secondary aerosol formation, *Biogeosciences*, 10(2), 653–667,  
1434 doi:10.5194/bg-10-653-2013, 2013.  
1435  
1436 Fuchs, N. A.: *Mechanics of Aerosols*, Pergamon, New York, 1964.  
1437  
1438 Garrett, T. J., Brattström, S., Sharma, S., Worthy, D. E. J. and Novelli, P.: The role of  
1439 scavenging in the seasonal transport of black carbon and sulfate to the Arctic, *Geophys.*  
1440 *Res. Lett.*, 38(16), doi:10.1029/2011GL048221, 2011.  
1441

1442 Garrett, T. J., Zhao, C. and Novelli, P. C.: Assessing the relative contributions of  
1443 transport efficiency and scavenging to seasonal variability in Arctic aerosol, *Tellus B*,  
1444 62(3), 190–196, doi:10.1111/j.1600-0889.2010.00453.x, 2010.

1445  
1446 Gettelman, A., Morrison, H., Terai, C. R. and Wood, R.: Microphysical process rates and  
1447 global aerosol-cloud interaction, *Atmos. Chem. Phys.*, 13, 9855-9867, 2013.

1448

1449 Ghan, S. J., Rissman, T. A., Elleman, R., Ferrare, R. A., Turner, D., Flynn, C., Wang, J.,  
1450 Ogren, J., Hudson, J., Jonsson, H. H., VanReken, T., Flagan, R. C. and Seinfeld, J. H.:  
1451 Use of in situ cloud condensation nuclei, extinction, and aerosol size distribution  
1452 measurements to test a method for retrieving cloud condensation nuclei profiles from  
1453 surface measurements, *J. Geophys. Res.*, 111(D5), 2006.

1454

1455 Giamarelou, M., Eleftheriadis, K., Nyeki, S., Tunved, P., Torseth, K. and Biskos, G.:  
1456 Indirect evidence of the composition of nucleation mode atmospheric particles in the high  
1457 Arctic, *J. Geophys. Res.*, 121, doi:10.1002/2015JD023646, 2016.

1458

1459 Giorgi, F. and Chameides, W. L.: Rainout Lifetimes of Highly Soluble Aerosols and  
1460 Gases as Inferred From Simulations With a General Circulation Model, *J. Geophys. Res.*,  
1461 91(D13), 14367–14376, 1986.

1462

1463 Haywood, J. M. and Boucher, O.: Estimates of the Direct and Indirect Radiative Forcing  
1464 Due to Tropospheric Aerosols: A review, *Rev. Geophys.*, (38), 513–543, 2000.

1465

1466 Heintzenberg, J., Leck, C. and Tunved, P.: Potential source regions and processes of  
1467 aerosol in the summer Arctic, *Atmos. Chem. Phys.*, 15(11), 6487–6502, doi:10.5194/acp-  
1468 15-6487-2015, 2015.

1469

1470 Herzog, M., Weisenstein, D. K. and Penner, J. E.: A dynamic aerosol module for global  
1471 chemical transport models: Model description, *J. Geophys. Res. Atmos.*, 109,  
1472 doi:10.1029/2003JD004405, 2004.

1473

1474 Hoose, C., Lohmann, U., Bennartz, R., Croft, B. and Lesins, G.: Global simulations of  
1475 aerosol processing in clouds, *Atmos. Chem. Phys. Discuss.*, 8(4), 13555–13618, 2008.

1476

1477 Kerminen, V. M., Anttila, T., Lehtinen, K. E. J. and Kulmala, M.: Parameterization for  
1478 atmospheric new-particle formation: Application to a system involving sulfuric acid and  
1479 condensable water-soluble organic vapors, *Aerosol Sci. Technol.*, 38(10), 1001–1008,  
1480 2004.

1481

1482 Korhonen, H., Carslaw, K. S., Spracklen, D. V., Ridley, D. A. and Ström, J.: A global  
1483 model study of processes controlling aerosol size distributions in the Arctic spring and  
1484 summer, *J. Geophys. Res.*, 113(D8), 1–20, doi:10.1029/2007JD009114, 2008.

1485

1486 Kristiansen, N. I., Stohl, A., Olivié, D. J. L., Croft, B., Søvde, O. A. and Klein, H.:  
1487 Evaluation of observed and modelled aerosol lifetimes using radioactive tracers of  
1488 opportunity and an ensemble of 19 global models, 24513–24585, doi:10.5194/acpd-15-  
1489 24513-2015, 2015.

1490

1491 [Leaitch, W. R., Korolev, A., Aliabadi, A., Burkhardt, J., Willis, M., Abbatt, J. P. D.,](#)  
1492 [Bozem, H., Hoor, P., Köllner, F., Schneider, J., Herber, A., Konrad, J., Brauner, R.:](#)  
1493 [Effects of 20-100 nanometre particle on liquid cloud in the clean summertime Arctic,](#)  
1494 [Atmos. Chem. Phys. Discuss. doi:10.5194/acp-2015-999, 2016.](#)

1495

1496 [Leaitch, W. R., Sharma, S., Huang, L., Toom-Sauntry, D., Chivulescu, A., Macdonald, A.](#)  
1497 [M., von Salzen, K., Pierce, J. R., Bertram, A. K., Schroder, J. C., Shantz, N. C., Chang,](#)  
1498 [R. Y. W. and Norman, A.-L.: Dimethyl sulfide control of the clean summertime Arctic](#)  
1499 [aerosol and cloud, Elem. Sci. Anth., 1, 17, doi:10.12952/journal.elementa.000017, 2013.](#)

1500

1501 [Lee, Y. H. and Adams, P. J.: A Fast and Efficient Version of the TwO-Moment Aerosol](#)  
1502 [Sectional \(TOMAS\) Global Aerosol Microphysics Model, Aerosol Sci. Technol., 46\(6\),](#)  
1503 [678–689, doi:10.1080/02786826.2011.643259, 2012.](#)

1504

1505 [Lee, Y.H., Pierce, J.R., Adams, P.J.: Representation of nucleation mode microphysics in](#)  
1506 [global aerosol microphysics models, Geosci. Model Dev., 6, 1221-1232,](#)  
1507 [doi:10.5194/gmd-6-1221-2013, 2013a.](#)

1508

1509 [Lee, L. A., Pringle, K. J., Reddington, C. L., Mann, G. W., Stier, P., Spracklen, D. V.,](#)  
1510 [Pierce, J. R. and Carslaw, K. S.: The magnitude and causes of uncertainty in global model](#)  
1511 [simulations of cloud condensation nuclei, Atmos. Chem. Phys., 13\(17\), 8879–8914,](#)  
1512 [doi:10.5194/acpd-13-6295-2013, 2013b.](#)

1513

1514 Liu, H., Jacob, D. J., Bey, I. and Yantosca, R. M.: Constraints from  $^{210}\text{Pb}$  and  $^7\text{Be}$  on  
1515 wet deposition and transport in a global three-dimensional chemical tracer model driven  
1516 by assimilated meteorological fields, *J. Geophys. Res.*, 106(D11), 12109–12128, 2001.  
1517

1518 Lohmann, U. and Feichter, J.: Global indirect aerosol effects: a review, *Atmos. Chem.*  
1519 *Phys. Discuss.*, 4, 7561–7614, doi:10.5194/acpd-4-7561-2004, 2004.  
1520

1521 Mann, G. W., Carslaw, K. S., Spracklen, D. V., Ridley, D. A., Manktelow, P. T.,  
1522 Chipperfield, M. P., Pickering, S. J. and Johnson, C. E.: Description and evaluation of  
1523 GLOMAP-mode: a modal global aerosol microphysics model for the UKCA  
1524 composition-climate model, *Geosci. Model Dev. Discuss.*, 3, 651–734,  
1525 doi:10.5194/gmdd-3-651-2010, 2010.  
1526

1527 Mann, G. W., Carslaw, K. S., Ridley, D. A., Spracklen, D. V., Pringle, K. J., Merikanto,  
1528 J., Korhonen, H., Schwarz, J. P., Lee, L. A., Manktelow, P. T., Woodhouse, M. T.,  
1529 Schmidt, A., Breider, T. J., Emmerson, K. M., Reddington, C. L., Chipperfield, M. P. and  
1530 Pickering, S. J.: Intercomparison of modal and sectional aerosol microphysics  
1531 representations within the same 3-D global chemical transport model, *Atmos. Chem.*  
1532 *Phys.*, 12, 4449–4476, doi:10.5194/acp-12-4449-2012, 2012.  
1533

1534 Möhler, O. and Arnold, F.: Gaseous sulfuric acid and sulfur dioxide measurements in the  
1535 Arctic troposphere and lower stratosphere: Implications for hydroxyl radical abundances,  
1536 *Geophys. Res. Lett.*, 19, 1763-1766, 1992.  
1537

1538 Napari, I., Noppel, M., Vehkamäki, H. and Kulmala, M.: Parameterization of ternary  
1539 nucleation rates for H<sub>2</sub>SO<sub>4</sub>-NH<sub>3</sub>-H<sub>2</sub>O vapors, *J. Geophys. Res.*, 107(D19), 4310–4381,  
1540 2002.  
1541  
1542 O’Dowd, C. D. and de Leeuw, G.: Marine aerosol production: a review of the current  
1543 knowledge., *Philos. Trans. A. Math. Phys. Eng. Sci.*, 365(1856), 1753–1774,  
1544 doi:10.1098/rsta.2007.2043, 2007.  
1545  
1546 Olenius, T., Kupiainen-Määttä, O., Ortega, I. K., Kurtén, T. and Vehkamäki, H.: Free  
1547 energy barrier in the growth of sulfuric acid-ammonia and sulfuric acid-dimethylamine  
1548 clusters, *J. Chem. Phys.*, 139(8), doi:10.1063/1.4819024, 2013.  
1549  
1550 Pierce, J.R., Adams, P.J., Uncertainty in global CCN concentrations from uncertain  
1551 aerosol nucleation and primary emission rates, *Atmospheric Chemistry and Physics*, 9,  
1552 1339-1356, 2009.  
1553  
1554 Pierce, J. R., Riipinen, I., Kulmala, M., Ehn, M., Petäjä, T., Junninen, H., Worsnop, D.  
1555 R., and Donahue, N. M.: Quantification of the volatility of secondary organic compounds  
1556 in ultrafine particles during nucleation events, *Atmos. Chem. Phys.*, 11, 9019-9036,  
1557 doi:10.5194/acp-11-9019-2011, 2011.  
1558  
1559 Pierce, J.R., Evans, M.J., Scott, C.E., D’Andrea, S.D., Farmer, D.K., Swietlicki, E.,  
1560 Spracklen, D.V.: Weak sensitivity of cloud condensation nuclei and the aerosol indirect

1561 effect to Criegee+SO<sub>2</sub> chemistry, *Atmospheric Chemistry and Physics*, 13, 3163-3176,  
1562 doi:10.5194/acp-13-3163-2013, 2013.

1563

1564 Pierce, J. R., Croft, B., Kodros, J. K., D'Andrea, S. D. and Martin, R. V.: The importance  
1565 of interstitial particle scavenging by cloud droplets in shaping the remote aerosol size  
1566 distribution and global aerosol-climate effects, *Atmos. Chem. Phys.*, 15(11), 6147–6158,  
1567 doi:10.5194/acp-15-6147-2015, 2015.

1568

1569 Riddick, S. N., Dragosits, U., Blackall, T. D., Daunt, F., Wanless, S. and Sutton, M. a.:  
1570 The global distribution of ammonia emissions from seabird colonies, *Atmos. Environ.*,  
1571 55, 319–327, doi:10.1016/j.atmosenv.2012.02.052, 2012.

1572

1573 Riipinen, I., Pierce, J. R., Yli-Juuti, T., Nieminen, T., Häkkinen, S., Ehn, M., Junninen,  
1574 H., Lehtipalo, K., Petäjä, T., Slowik, J., Chang, R., Shantz, N. C., Abbatt, J., Leitch, W.  
1575 R., Kerminen, V.-M., Worsnop, D. R., Pandis, S. N., Donahue, N. M. and Kulmala, M.:  
1576 Organic condensation: a vital link connecting aerosol formation to cloud condensation  
1577 nuclei (CCN) concentrations, *Atmos. Chem. Phys.*, 11, 3865-3878, doi:10.5194/acp-11-  
1578 3865-2011, 2011.

1579

1580 Seabird Information Network: Circumpolar Seabird Data Portal, [online] Available from:  
1581 [http://axiom.seabirds.net/circumpolar\\_portal.php](http://axiom.seabirds.net/circumpolar_portal.php) (Accessed 13 March 2015), 2015.

1582

1583 Sharma, S., Ishizawa, M., Chan, D., Lavoué, D., Andrews, E., Eleftheriadis, K. and  
1584 Maksyutov, S.: 16-year simulation of Arctic black carbon: Transport, source contribution,

1585 and sensitivity analysis on deposition, *J. Geophys. Res. Atmos.*, 118(2), 943–964,  
1586 doi:10.1029/2012JD017774, 2013.

1587

1588 Shindell, D. and Faluvegi, G.: Climate response to regional radiative forcing during the  
1589 twentieth century, *Nature Geosci.*, 2, 294–300, doi:10.1038/NGEO473, 2009.

1590

1591 Shupe, M. D., Uttal, T., Matrosov, S. Y. and Frisch, A. S.: Cloud Water Contents and  
1592 Hydrometeor Sizes During the FIRE Arctic Clouds Experiment, *J. Geophys. Res.*,  
1593 106(D14), 15015–15028, 2001.

1594

1595 Spracklen, D. V, Pringle, K. J., Carslaw, K. S., Chipperfield, M. P. and Mann, G. W.: A  
1596 global off-line model of size-resolved aerosol microphysics: I. Model development and  
1597 prediction of aerosol properties, *Atmos. Chem. Phys.*, 5, 2227–2252, 2005a.

1598

1599 Spracklen, D. V, Pringle, K. J., Carslaw, K. S., Chipperfield, M. P. and Mann, G. W.: A  
1600 global off-line model of size-resolved aerosol microphysics: II. Identification of key  
1601 uncertainties, *Atmos. Chem. Phys.*, 5, 3233–3250, 2005b.

1602

1603 Spracklen, D. V, Carslaw, K. S., Kulmala, M., Kerminen, V. M., Sihto, S. L., Riipinen, I.,  
1604 Merikanto, J., Mann, G. W., Chipperfield, M. P., Wiedensohler, A., Birmili, W. and  
1605 Lihavainen, H.: Contribution of particle formation to global cloud condensation nuclei  
1606 concentrations, *Geophys. Res. Lett.*, 35(6), D06808, doi:10.1029/2007GL033038, 2008.

1607

1608 Stevens, R. G. and Pierce, J. R.: The contribution of plume-scale nucleation to global and  
1609 regional aerosol and CCN concentrations: evaluation and sensitivity to emissions  
1610 changes, *Atmos. Chem. Phys. Discuss.*, 14, 21473-21521, doi:10.5194/acpd-14-21473-  
1611 2014, 2014.

1612

1613 Stohl, A., Klimont, Z., Eckhardt, S., Kupiainen, K., Shevchenko, V. P., Kopeikin, V. M.  
1614 and Novigatsky, A. N.: Black carbon in the Arctic: the underestimated role of gas flaring  
1615 and residential combustion emissions, *Atmos. Chem. Phys.*, 13(17), 8833–8855,  
1616 doi:10.5194/acp-13-8833-2013, 2013.

1617 Ström, J., Umegard, J., Torseth, K., Tunved, P., Hansson, H. C., Holmen, K., Wismann,  
1618 V., Herber, A., and König-Langlo, G.: One year of particle size distribution and aerosol  
1619 chemical composition measurements at the Zeppelin Station, Svalbard, March 2000–  
1620 March 2001, *Phys. Chem. Earth*, 28, 1181–1190, doi:10.1016/j.pce.2003.08.058, 2003.

1621

1622 Trivitayanurak, W., Adams, P. J., Spracklen, D., and Carslaw, K. S.: Tropospheric  
1623 aerosol microphysics simulation with assimilated meteorology: model description and  
1624 intermodel comparison, *Atmospheric Chemistry and Physics*, 8(12), 3149–3168, 2008.

1625

1626 Tunved, P., Ström, J. and Hansson, H.-C.: An investigation of processes controlling the  
1627 evolution of the boundary layer aerosol size distribution properties at the Swedish  
1628 background station Aspöreten, *Atmos. Chem. Phys. Discuss.*, 4(4), 4507–4543,  
1629 doi:10.5194/acpd-4-4507-2004, 2004.

1630

1631 Tunved, P., Ström, J. and Krejci, R.: Arctic aerosol life cycle: linking aerosol size  
1632 distributions observed between 2000 and 2010 with air mass transport and precipitation at  
1633 Zeppelin station, Ny-Ålesund, Svalbard, *Atmos. Chem. Phys.*, 13(7), 3643–3660,  
1634 doi:10.5194/acp-13-3643-2013, 2013.

1635

1636 Twomey, S.: Pollution and the Planetary Albedo, *Atmos. Environ.*, 8, 1251–1256, 1974.

1637

1638 Vehkamäki, H., Kulmala, M., Napari, I., Lehtinen, K. E. J., Timmreck, C., Noppel, M.  
1639 and Laaksonen, A.: An improved parameterization for sulfuric acid-water nucleation  
1640 rates for tropospheric and stratospheric conditions, *J. Geophys. Res.*, 107(D22), 4610–  
1641 4622, 2002.

1642

1643 Verheggen, B., Cozic, J., Weingartner, E., Bower, K., Mertes, S., Connolly, P.,  
1644 Gallagher, M., Flynn, M., Choulaton, T. and Baltensperger, U.: Aerosol partitioning  
1645 between the interstitial and the condensed phase in mixed-phase clouds, *J. Geophys. Res.*,  
1646 112(D23), D23202, doi:10.1029/2007JD008714, 2007.

1647

1648 Wang, M. and Penner, J. E.: Aerosol indirect forcing in a global model with particle  
1649 nucleation, *Atmos. Chem. Phys.*, 9(1), 239–260, doi:10.5194/acp-9-239-2009, 2009.

1650

1651 Wang, Q., Jacob, D. J., Fisher, J. a., Mao, J., Leibensperger, E. M., Carouge, C. C., Le  
1652 Sager, P., Kondo, Y., Jimenez, J. L., Cubison, M. J. and Doherty, S. J.: Sources of  
1653 carbonaceous aerosols and deposited black carbon in the Arctic in winter-spring:

1654 implications for radiative forcing, *Atmos. Chem. Phys.*, 11(23), 12453–12473,  
1655 doi:10.5194/acp-11-12453-2011, 2011.

1656

1657 **Wentworth, G. R., Murphy, J. G., Croft, B., Martin, R. V., Pierce, J. R., Cote, J.-S.,**  
1658 **Courchesne, I., Tremblay, J.-E., Gagnon, J., Thomas, J. L., Sharma, S., Toom-Saunty,**  
1659 **D., Chivulescu, A., Levasseur, M., and Abbatt, J. P. D.: Ammonia in the summertime**  
1660 **Arctic marine boundary layer: Sources, sinks and implications, *Atmos. Chem. Phys.*, 16,**  
1661 **1937-1953, doi:10.5194/acp-16-1937-2016, 2016.**

1662

1663 Westervelt, D. M., Pierce, J. R., Riipinen, I., Trivitayanurak, W., Hamed, A., Kulmala,  
1664 M., Laaksonen, A., Decesari, S., and Adams, P. J.: Formation and growth of nucleated  
1665 particles into cloud condensation nuclei: model-measurement comparison, *Atmos. Chem.*  
1666 *Phys.*, 13, 7645–7663, doi:10.5194/acp-13-7645-2013, 2013.

1667

1668 Williams, J., de Reus, M., Krejci, R., Fischer, H. and Ström, J.: Application of the  
1669 variability-size relationship to atmospheric aerosol studies: estimating aerosol lifetimes  
1670 and ages, *Atmos. Chem. Phys.*, 2(1), 43–74, doi:10.5194/acpd-2-43-2002, 2002.

1671

1672 Yu, F. and Luo, G.: Simulation of particle size distribution with a global aerosol model:  
1673 contribution of nucleation to aerosol and CCN number concentrations, *Atmos. Chem.*  
1674 *Phys. Discuss.*, 9, 10597–10645, doi:10.5194/acpd-9-10597-2009, 2009.

1675

1676 Yu, F.: A secondary organic aerosol formation model considering successive oxidation  
1677 aging and kinetic condensation of organic compounds: Global scale implications, *Atmos.*  
1678 *Chem. Phys.*, 11, 1083–1099, doi:10.5194/acp-11-1083-2011, 2011.

1679

1680

1681 **Figure Captions:**

1682

1683

1684 Figure 1: Measured monthly median number distributions from the scanning mobility  
1685 particle sizer (SMPS) at Alert for 2011-2013 and the differential mobility particle sizer  
1686 (DMPS) at Mt. Zeppelin for 2011-2013 for particle sizes between 20 nm and 500 nm.  
1687 Error bars show the 20-80th percentile of the measurements.

1688

1689

1690 Figure 2: Measurement monthly median aerosol effective diameter from SMPS and  
1691 DMPS at the two high-Arctic sites, Alert (2011-2013) and Mt. Zeppelin (2011-2013),  
1692 respectively, for particle sizes between 20 nm and 500 nm. Error bars show the 20th and  
1693 80th percentiles.

1694

1695 Figure 3: Seasonal median number distributions from SMPS measurements at Alert  
1696 (2011-2013) and for the GEOS-Chem-TOMAS dry size distribution  
1697 simulations (described in Table 1). The measurement 20-80th percentile is in grey  
1698 shading. Simulations are shown in color as indicated by legend.

1699

1700 Figure 4: Seasonal median number distributions from DMPS measurements at Mt.  
1701 Zeppelin (2011-2013) and for the GEOS-Chem-TOMAS dry size distribution simulations

1702 (described in Table 1). The measurement 20-80th percentile is in grey shading.

1703 Simulations are shown in color as indicated by legend.

1704

1705 Figure 5: Monthly median number concentration for aerosols with diameters of 20-500

1706 nm (N20), 80-500 nm (N80), and 200-500 nm (N200), and effective diameter from the

1707 2011-2013 Alert SMPS measurements and for the four GEOS-Chem-TOMAS dry size

1708 distribution simulations described in Table 1. The measurement 20-80th percentile is in

1709 grey shading. Simulations are shown in color as indicated by legend.

1710

1711 Figure 6: Monthly median number concentration for aerosols with diameters of 20-500

1712 nm (N20), 80-500 nm (N80), and 200-500 nm (N200), and effective diameter from the

1713 2011-2013 Mt. Zeppelin DMPS measurements and for the four GEOS-Chem-TOMAS

1714 dry size distribution simulations described in Table 1. The measurement 20-80th

1715 percentile is in grey shading. Simulations are shown in color as indicated by legend.

1716

1717 Figure 7: Geographic distribution of the simulated pan-Arctic surface-layer seasonal-

1718 mean dry effective diameter [nm] for the NEWS-CAV+COAG simulation. The coloured

1719 stars indicate the effective diameter from measurements at Alert (SMPS) and Mt.

1720 Zeppelin (DMPS).

1721

1722 Figure 8: Monthly and Arctic mean aerosol number process rates for the entire Arctic

1723 troposphere (north of 66°N) for simulation NEWS-CAV+COAG. Processes considered

1724 for each of four size ranges are condensation, coagulation, particle formation, primary

1725 emissions, wet and dry deposition, transport across 66 °N and net regional buildup or loss  
1726 rates. The aerosol size ranges are nucleation ( $D_p < 10$  nm), Aitken ( $10 < D_p < 100$  nm),  
1727 accumulation ( $100 < D_p < 1000$  nm), and coarse ( $D_p > 1000$  nm).

1728

1729 Figure 9: Monthly and Arctic mean aerosol number tendency due to transport within each  
1730 of four vertical layers between 1) 0-1.5 km, 2) 1.5-4 km, 3) 4-10 km, and 4) above 10 km  
1731 for the simulation NEWS-CAV+COAG for the entire troposphere north of 66°N.

1732 Summation of the 4 layers for any given month and size range yields the transport  
1733 tendency shown in Fig.8. Positive values indicate a net northward transport into the  
1734 Arctic.

1735

1736

1737 Figure 10: Regional and monthly mean aerosol number lifetime with respect to wet  
1738 deposition for accumulation-mode aerosol number ( $100 < D_p < 1000$  nm) and in the altitude  
1739 bands of 0-1.5 km, and 1.5-4 km for the GEOS-Chem simulation NEWS-CAV+COAG.

1740

1741 Figure 11: Monthly- and regional-mean aerosol number process rates for the entire  
1742 troposphere north of 50°N for simulation NEWS-CAV+COAG. Processes considered for  
1743 each of four size ranges are nucleation, emissions, coagulation, condensation, wet and dry  
1744 deposition, transport across 66°N and net regional accumulation or loss rates. The aerosol  
1745 size ranges are nucleation ( $D_p < 10$  nm), Aitken ( $10 < D_p < 100$  nm),  
1746 accumulation ( $100 < D_p < 1000$  nm), and coarse ( $D_p > 1000$  nm).

1747

1748

1749  
1750  
1751  
1752  
1753

**Tables:**

Table 1: Summary of the simulations conducted for this study.

Simulation Name	Revised Wet Removal	With Interstitial Coagulation	With New-Particle Formation
STD	no	no	yes
NEWSCAV	yes	no	yes
NEWSCAV+COAG	yes	yes	yes
NONUC	yes	no	no

1754  
1755

1756  
1757  
1758

Table 2: Model-measurement fractional bias (Eq. 6) for total number of aerosols with diameters of 20-100 nm and 100-500 nm at Alert (in reference to Fig. 3). Bias values closest to zero for each season are highlighted in red.

1759  
1760  
1761  
1762

Bias	STD	NEWSCAV	NEWSCAV+COAG	NONUC
<b>20-100 nm</b>				
Winter	1.95	3.45	<b>0.18</b>	1.47
Spring	0.83	1.12	-0.46	<b>-0.36</b>
Summer	-0.58	0.56	<b>0.23</b>	-0.92
Fall	0.15	3.53	0.52	<b>0.07</b>
<b>100-500nm</b>				
Winter	0.66	0.87	0.40	<b>0.34</b>
Spring	0.38	0.30	<b>-0.01</b>	-0.40
Summer	0.98	0.21	<b>0.05</b>	-0.43
Fall	0.40	1.34	0.78	<b>0.01</b>

1763  
1764  
1765  
1766  
1767  
1768  
1769

1770 Table 3: Model-measurement fractional bias (Eq. 6) for total number of aerosols with  
 1771 diameters of 20-100 nm and 100-500 nm at Mt. Zeppelin (in reference to Fig. 4). Bias  
 1772 values closest to zero for each season are highlighted in red.  
 1773

Bias	STD	NEWSCAV	NEWSCAV+COAG	NONUC
<b>20-100 nm</b>				
Winter	6.73	12.87	<b>3.17</b>	5.43
Spring	0.68	1.01	<b>-0.40</b>	-0.43
Summer	-0.65	<b>-0.21</b>	-0.54	-0.90
Fall	0.34	4.59	1.14	<b>0.10</b>
<b>100-500nm</b>				
Winter	3.24	3.42	2.18	<b>2.09</b>
Spring	0.96	0.49	<b>0.19</b>	-0.22
Summer	0.60	<b>0.02</b>	-0.15	-0.61
Fall	1.50	1.63	0.99	<b>0.12</b>

1774  
 1775  
 1776  
 1777  
 1778  
 1779  
 1780  
 1781  
 1782  
 1783  
 1784

Table 4: Model-measurement mean fractional bias and mean fractional error (Eqs. 7 and 8) for N20, N80, N200 and effective diameter at Alert (in reference to Fig. 5). Bias and error values closest to zero for each season are highlighted in red.

	STD	NEWSCAV	NEWSCAV+COAG	NONUC
<b>MFB</b>				
N20	0.22	0.57	<b>0.06</b>	-0.53
N80	0.24	0.36	<b>0.05</b>	-0.43
N200	0.74	0.24	0.27	<b>0.17</b>
Eff. Diam.	0.17	<b>-0.05</b>	<b>0.05</b>	0.21
<b>MFE</b>				
N20	0.45	0.57	<b>0.23</b>	0.80
N80	0.32	0.37	<b>0.23</b>	0.60
N200	0.74	0.30	0.30	<b>0.29</b>
Eff. Diam.	0.20	0.10	<b>0.08</b>	0.22

1785  
 1786  
 1787  
 1788  
 1789  
 1790

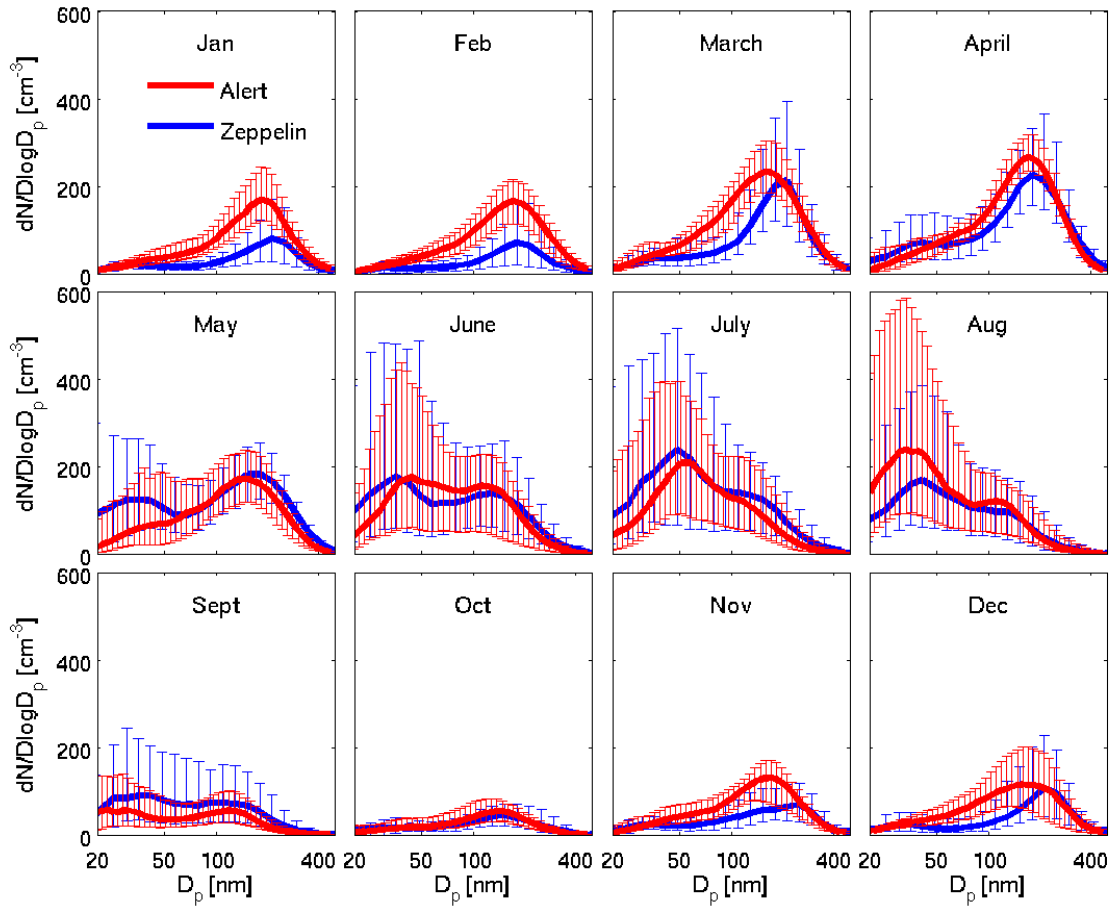
1791 Table 5: Model-measurement mean fractional bias and mean fractional error (Eqs. 7 and  
 1792 8) for N20, N80, N200 and effective diameter at Mt. Zeppelin (in reference to Fig. 6).  
 1793 Bias and error values closest to zero for each season are highlighted in red.  
 1794

	STD	NEWSCAV	NEWSCAV+COAG	NONUC
<b>MFB</b>				
N20	0.46	0.66	0.21	<b>-0.18</b>
N80	0.65	0.57	0.31	<b>-0.11</b>
N200	0.86	0.20	0.22	<b>0.12</b>
Eff. Diam.	<b>0.04</b>	-0.17	-0.07	0.06
<b>MFE</b>				
N20	0.76	0.86	<b>0.75</b>	1.03
N80	<b>0.68</b>	0.77	<b>0.68</b>	0.88
N200	0.86	0.66	<b>0.54</b>	0.56
Eff. Diam.	0.12	0.17	<b>0.10</b>	0.17

1795  
 1796  
 1797  
 1798  
 1799  
  
 1800  
  
 1801  
  
 1802  
  
 1803  
  
 1804  
  
 1805  
  
 1806  
  
 1807  
  
 1808  
  
 1809  
  
 1810

1811 **Figures:**

1812 Figure 1: Measured monthly median number distributions from the scanning mobility  
1813 particle sizer (SMPS) at Alert for 2011-2013 and the differential mobility particle sizer  
1814 (DMPS) at Mt. Zeppelin for 2011-2013 for particle sizes between 20 nm and 500 nm.  
1815 Error bars show the 20-80th percentile of the measurements.



1816

1817

1818

1819

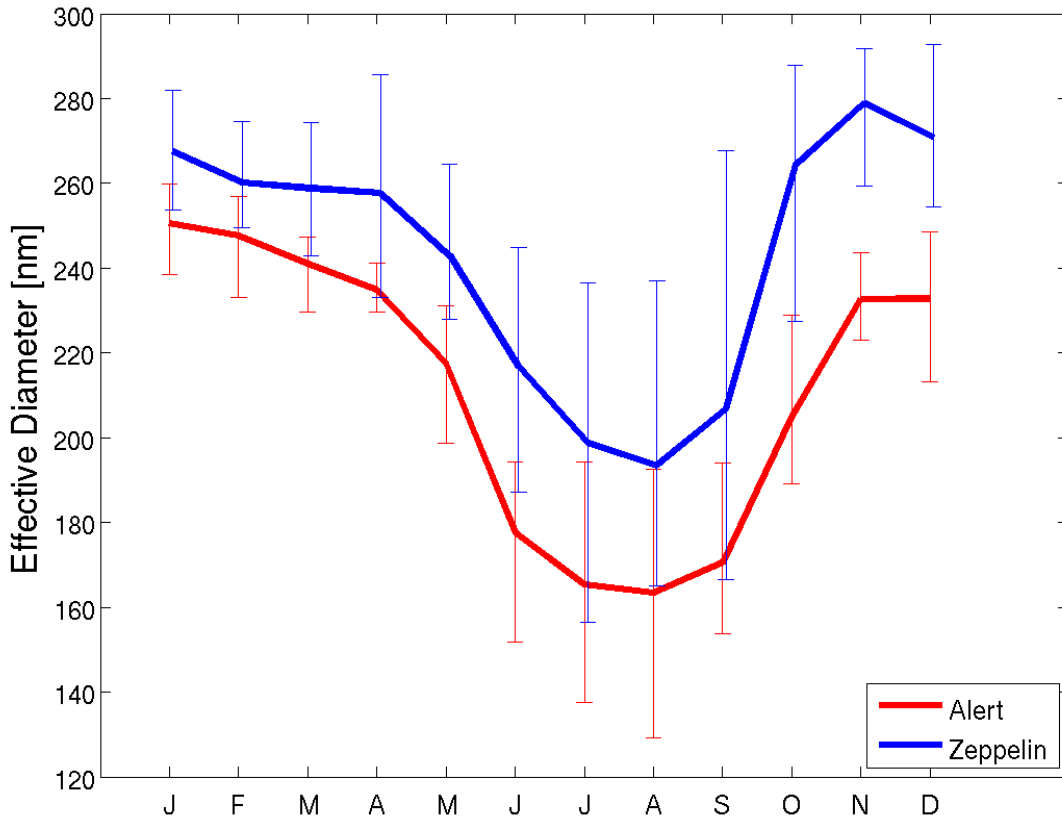
1820

1821

1822

1823

1824 Figure 2: Measurement monthly median aerosol effective diameter from SMPS and  
1825 DMPS at the two high-Arctic sites, Alert (2011-2013) and Mt. Zeppelin (2011-2013),  
1826 respectively, for particle sizes between 20 nm and 500 nm. Error bars show the 20th and  
1827 80th percentiles.



1828

1829

1830

1831

1832

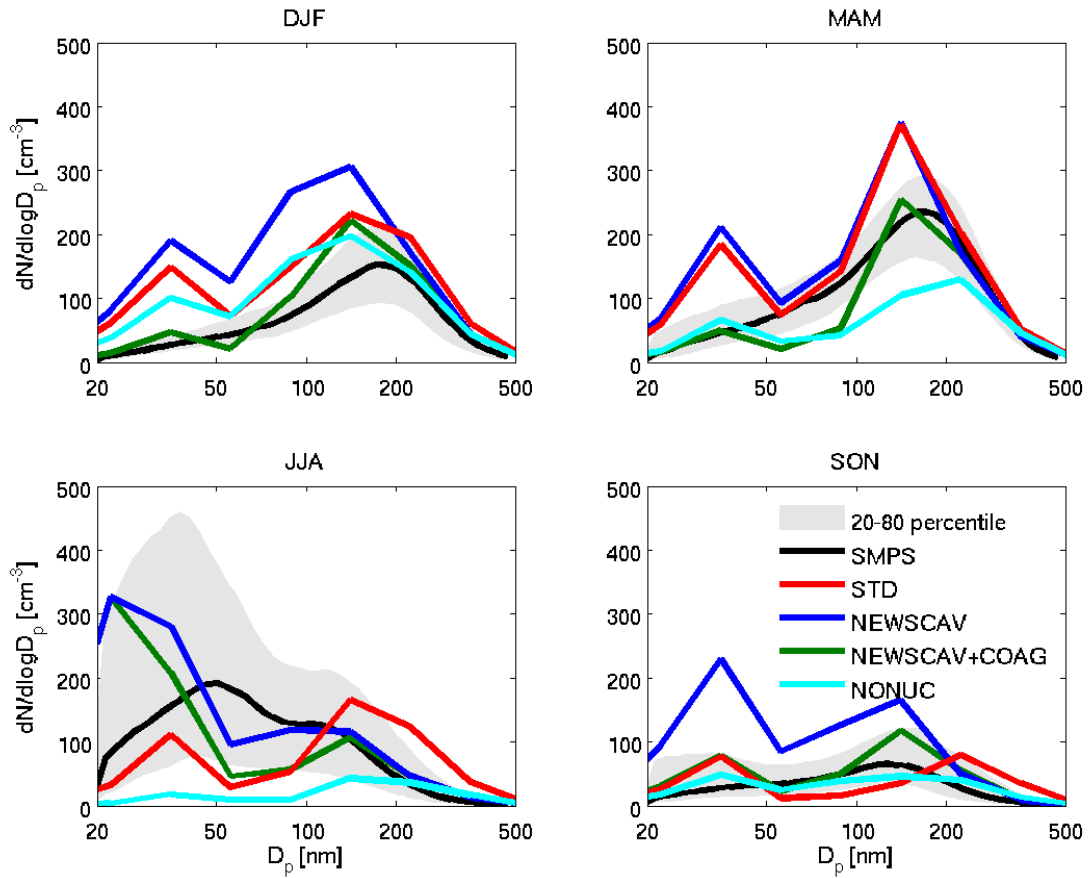
1833

1834

1835

1836

1837 Figure 3: Seasonal median number distributions from SMPS measurements at Alert  
1838 (2011-2013) and for the GEOS-Chem-TOMAS dry size distribution simulations  
1839 (described in Table 1). The measurement 20-80th percentile is in grey shading.  
1840 Simulations are shown in color as indicated by legend.



1841

1842

1843

1844

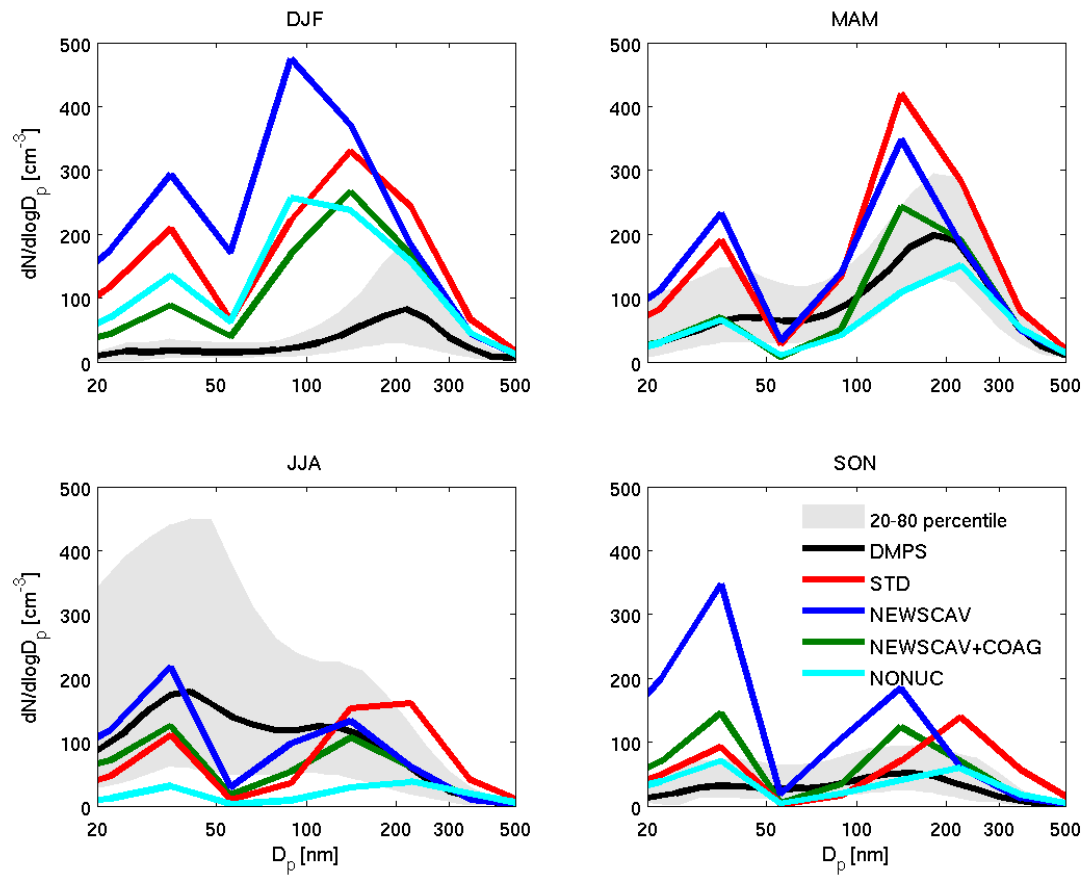
1845

1846

1847

1848

1849 Figure 4: Seasonal median number distributions from DMPS measurements at Mt.  
1850 Zeppelin (2011-2013) and for the GEOS-Chem-TOMAS dry size distribution simulations  
1851 (described in Table 1). The measurement 20-80th percentile is in grey shading.  
1852 Simulations are shown in color as indicated by legend.



1853

1854

1855

1856

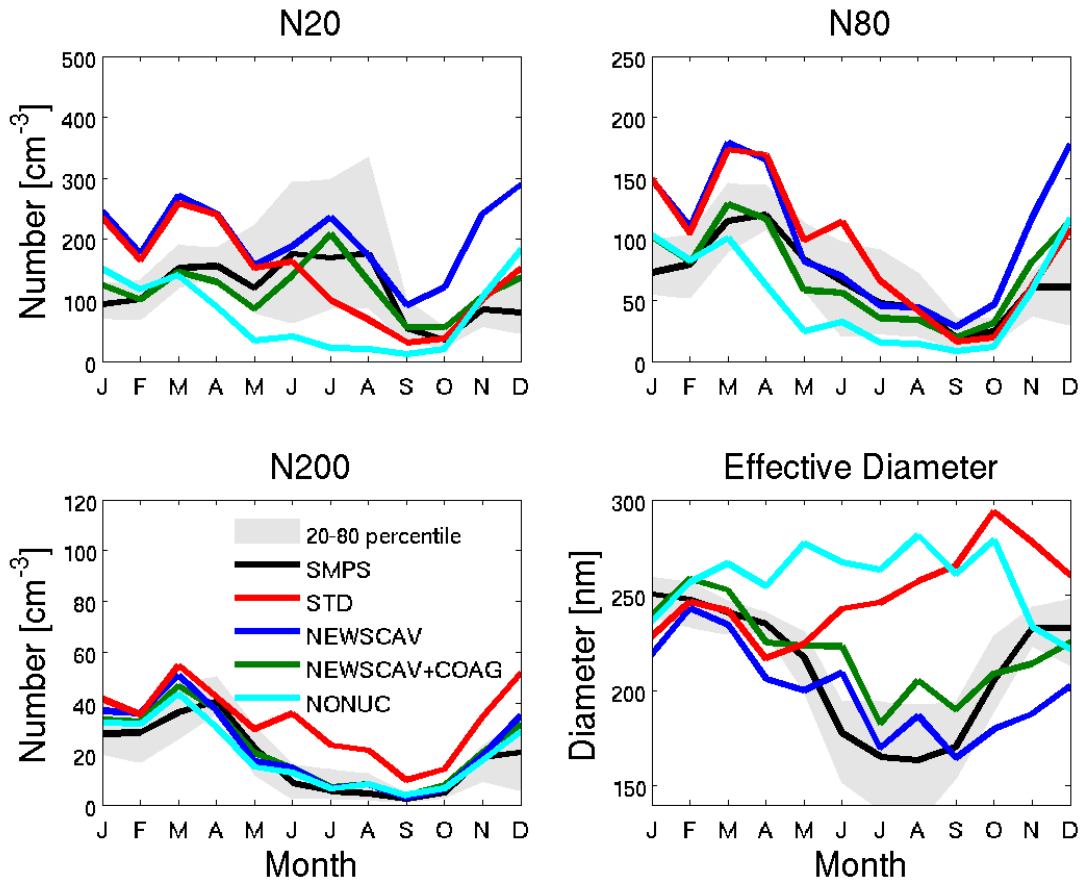
1857

1858

1859

1860

1861 Figure 5: Monthly median number concentration for aerosols with diameters of 20-500  
1862 nm (N20), 80-500 nm (N80), and 200-500 nm (N200), and effective diameter from the  
1863 2011-2013 Alert SMPS measurements and for the four GEOS-Chem-TOMAS dry size  
1864 distribution simulations described in Table 1. The measurement 20-80th percentile is in  
1865 grey shading. Simulations are shown in color as indicated by legend.



1866

1867

1868

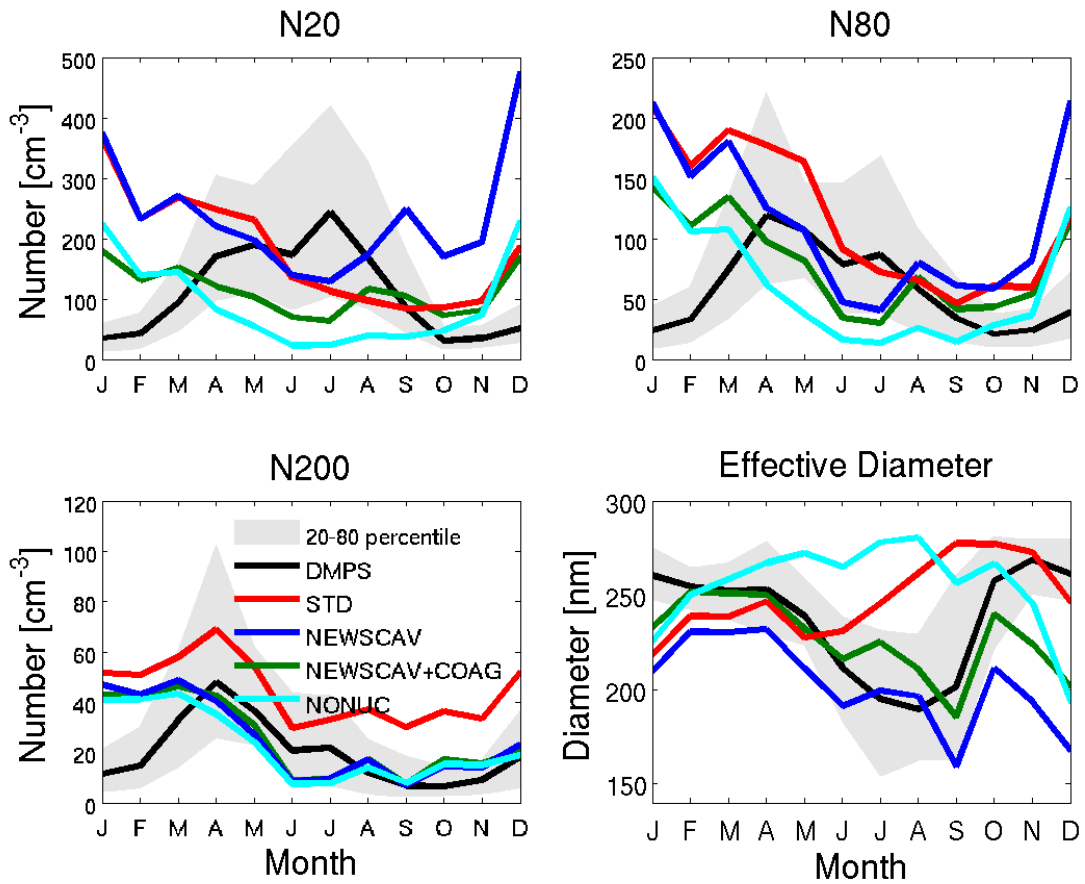
1869

1870

1871

1872

1873 Figure 6: Monthly median number concentration for aerosols with diameters of 20-500  
 1874 nm (N20), 80-500 nm (N80), and 200-500 nm (N200), and effective diameter from the  
 1875 2011-2013 Mt. Zeppelin DMPS measurements and for the four GEOS-Chem-TOMAS  
 1876 dry size distribution simulations described in Table 1. The measurement 20-80th  
 1877 percentile is in grey shading. Simulations are shown in color as indicated by legend.



1878

1879

1880

1881

1882

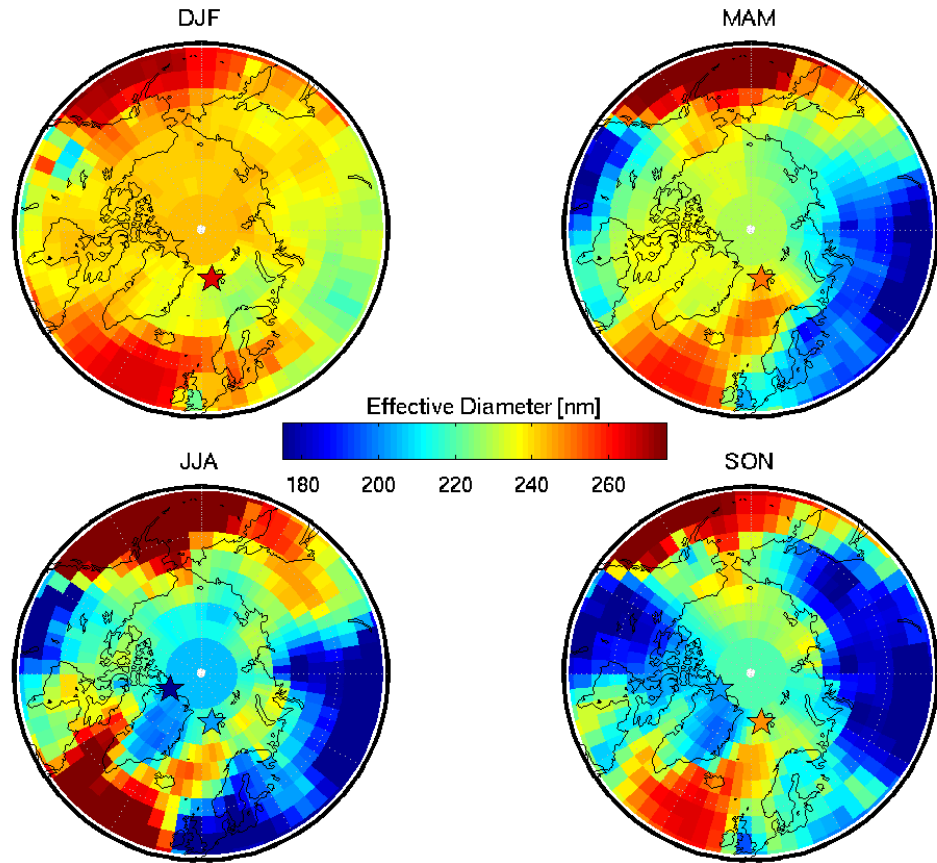
1883

1884

1885

1886

1887 Figure 7: Geographic distribution of the simulated pan-Arctic surface-layer  
1888 seasonal-mean dry effective diameter [nm] for the NEWSCAV+COAG simulation. The  
1889 colored stars indicate the effective diameter from measurements at Alert (SMPS) and Mt.  
1890 Zeppelin (DMPS).



1891

1892

1893

1894

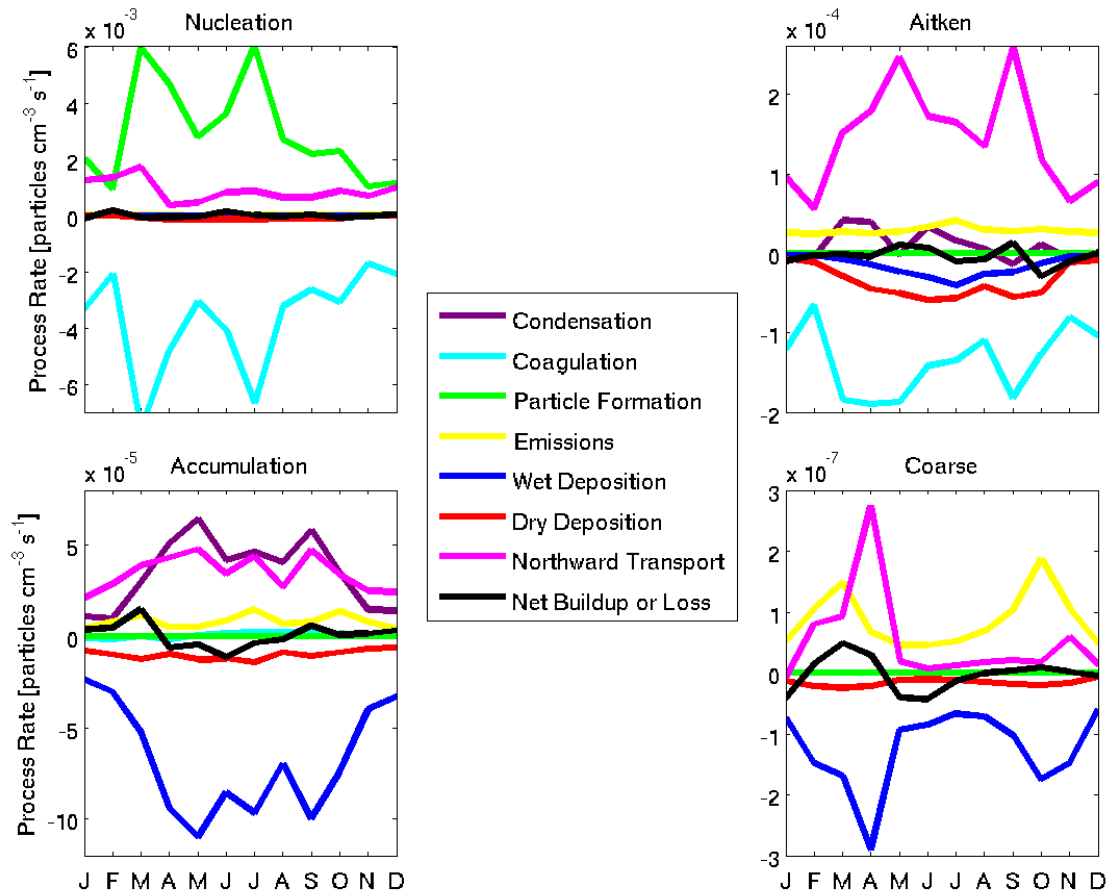
1895

1896

1897

1898

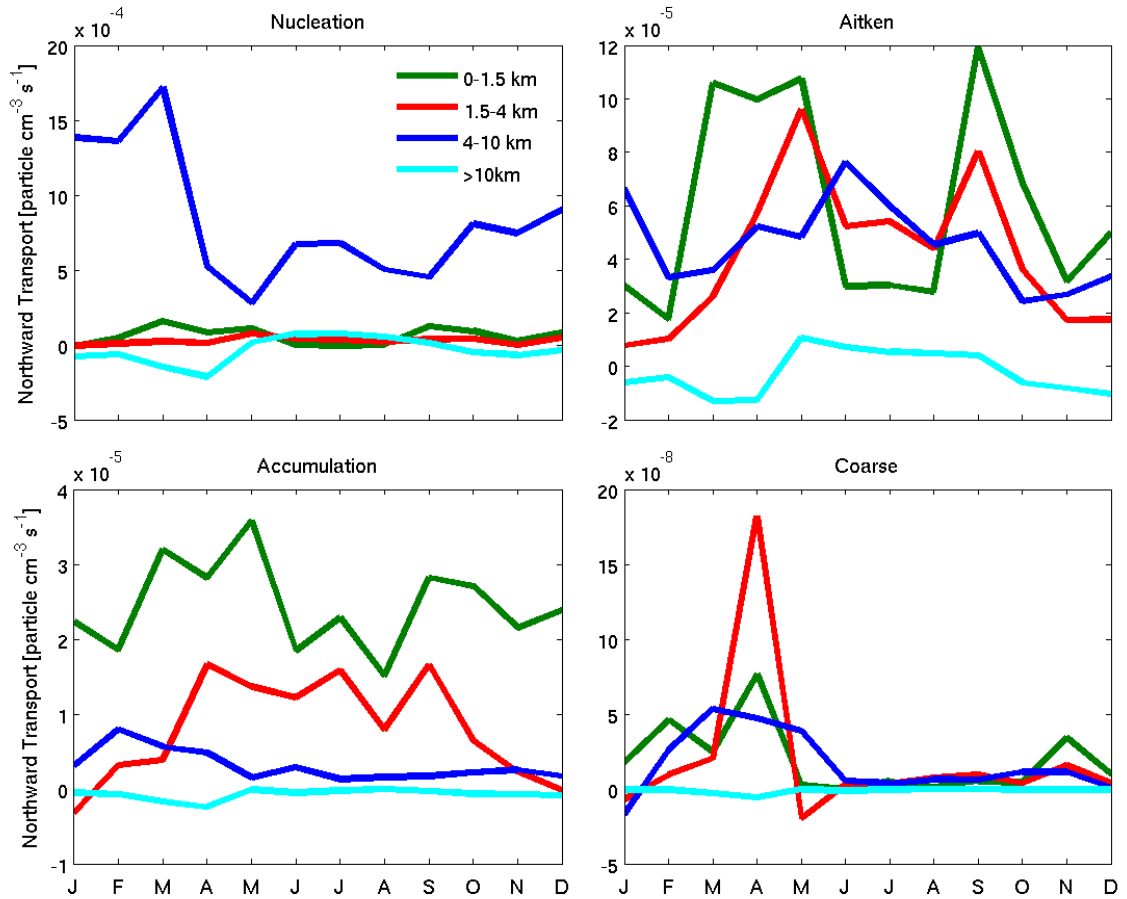
1899 Figure 8: Monthly and Arctic mean aerosol number process rates for the entire Arctic  
 1900 troposphere (north of 66°N) for simulation NEWS-CAV+COAG. Processes considered  
 1901 for each of four size ranges are condensation, coagulation, particle formation, primary  
 1902 emissions, wet and dry deposition, transport across 66 °N and net regional buildup or loss  
 1903 rates. The aerosol size ranges are nucleation ( $D_p < 10$  nm), Aitken ( $10 < D_p < 100$  nm),  
 1904 accumulation ( $100 < D_p < 1000$  nm), and coarse ( $D_p > 1000$  nm).



1905  
 1906  
 1907  
 1908  
 1909  
 1910  
 1911

1912

1913 Figure 9: Monthly and Arctic mean aerosol number tendency due to transport within each  
1914 of four vertical layers between 1) 0-1.5 km, 2) 1.5-4 km, 3) 4-10 km, and 4) above 10 km  
1915 for the simulation NEWSCAV+COAG for the entire troposphere north of 66°N.  
1916 Summation of the 4 layers for any given month and size range yields the transport  
1917 tendency shown in Fig.8. Positive values indicate a net northward transport into the  
1918 Arctic.



1919

1920

1921

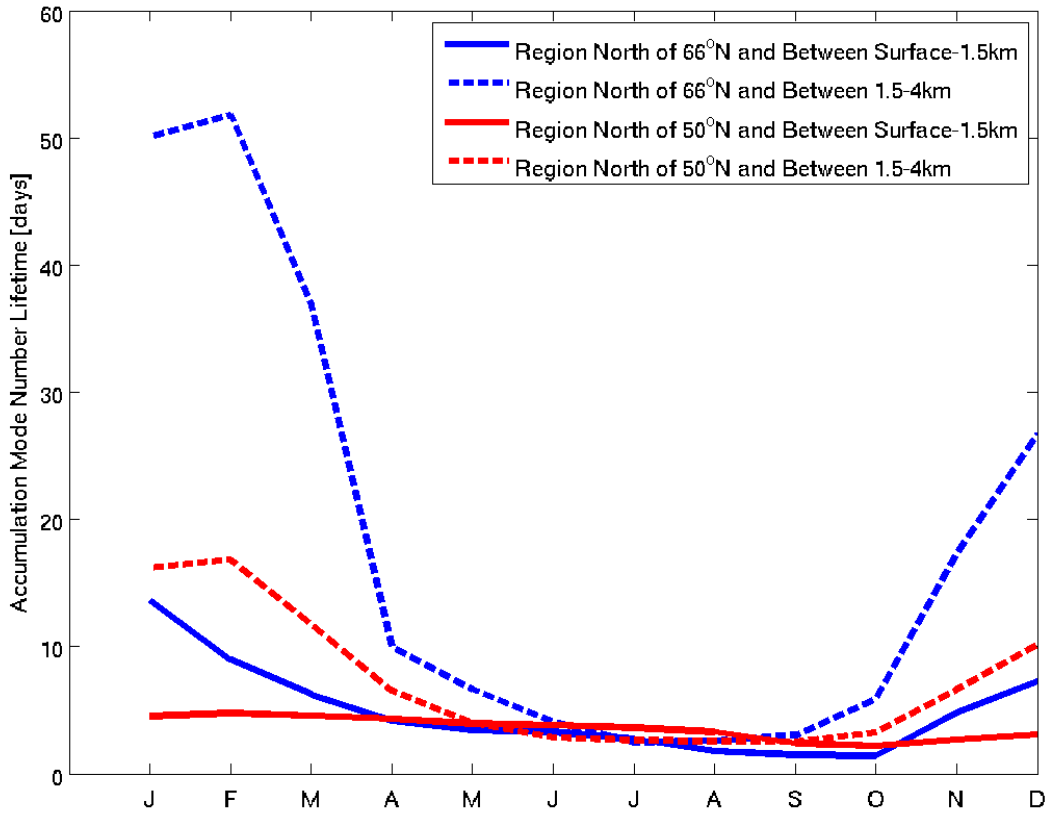
1922

1923

1924

1925

1926 Figure 10: Regional and monthly mean aerosol number lifetime with respect to wet  
 1927 deposition for accumulation-mode aerosol number ( $100 < D_p < 1000$  nm) in the altitude  
 1928 bands of 0-1.5 km, and 1.5-4 km for the GEOS-Chem simulation NEWS-CAV+COAG.



1929

1930

1931

1932

1933

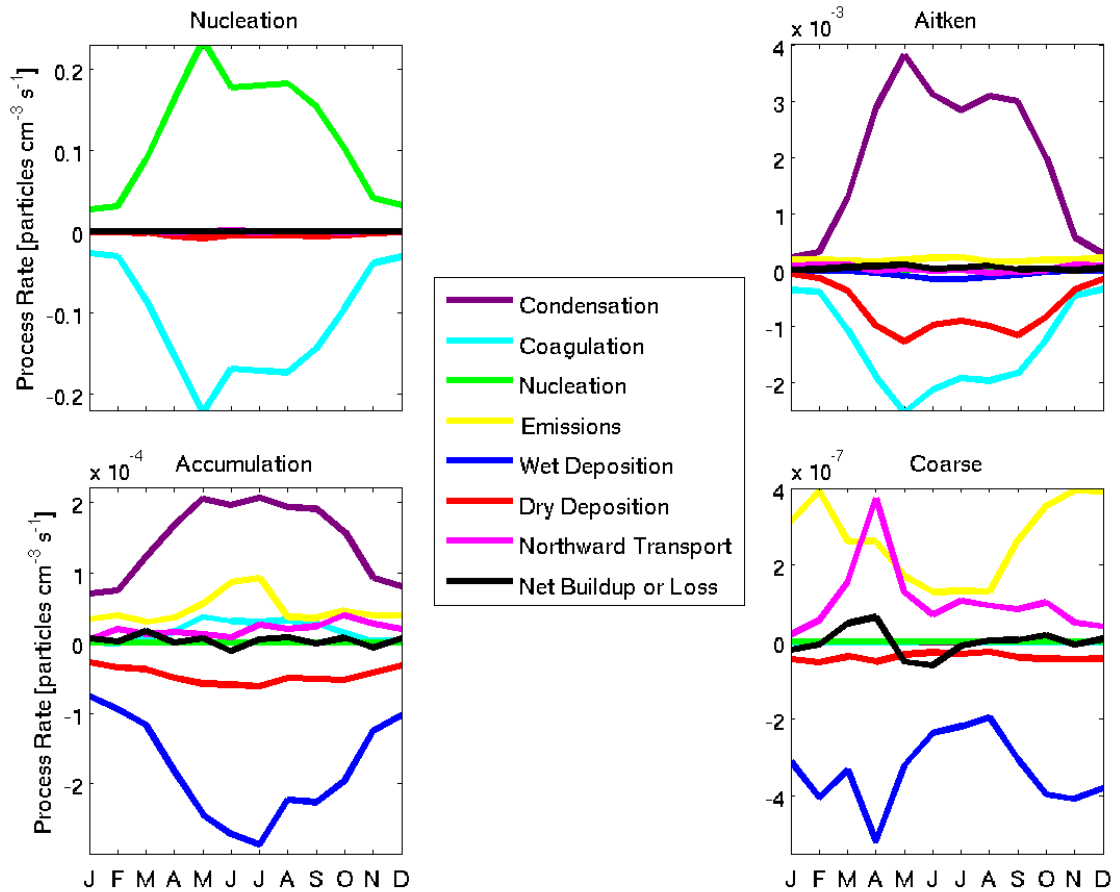
1934

1935

1936

1937

1938 Figure 11: Monthly and Arctic mean aerosol number process rates for the entire  
 1939 troposphere north of 50°N for simulation NEWS-CAV+COAG. Processes considered for  
 1940 each of four size ranges are nucleation, emissions, coagulation, condensation, wet and dry  
 1941 deposition, transport across 66°N and net regional accumulation or loss rates. The aerosol  
 1942 size ranges are nucleation ( $D_p < 10$  nm), Aitken ( $10 < D_p < 100$  nm), accumulation  
 1943 ( $100 < D_p < 1000$  nm), and coarse ( $D_p > 1000$  nm).



1944

